UC Berkeley
UC Berkeley Electronic Theses and Dissertations

Title
On Exotic Lagrangian Tori in CP2

Permalink
https://escholarship.org/uc/item/9cv1z769

Author
Vianna, Renato Ferreira de Velloso

Publication Date
2014

Peer reviewed|Thesis/dissertation

On Exotic Lagrangian Tori in $\mathbb{CP}^2$

by

Renato Ferreira de Velloso Vianna

A dissertation submitted in partial satisfaction of the
requirements for the degree of
Doctor of Philosophy

in

Mathematics

in the

Graduate Division

of the

University of California, Berkeley

Committee in charge:

Professor Denis Auroux, Chair
Professor Michael Hutchings
Professor Ian Agol
Professor Jonathan Wurtele

Spring 2014

On Exotic Lagrangian Tori in $\mathbb{CP}^2$

Abstract

On Exotic Lagrangian Tori in $\mathbb{CP}^2$

by

Renato Ferreira de Velloso Vianna

Doctor of Philosophy in Mathematics

University of California, Berkeley

Professor Denis Auroux, Chair

We construct an exotic monotone Lagrangian torus in $\mathbb{CP}^2$ using techniques motivated by mirror symmetry. We show that it bounds 10 families of Maslov index 2 holomorphic discs, and it follows that this exotic torus is not Hamiltonian isotopic to the known Clifford and Chekanov tori.

Para mãe, pai, vó Adélia, tia Bia, Ivana, Mariana, Spiff, Bruce, Zara, Argus, Ariel, a família Ajax, destacando Batata, Balaio, Seco, Thomás, Marcelo, Prot, Ceara e Teti, demais amigos de Brasília, em especial, Thiaguinho, Duds, Milhomem, Gabriel, Pedrão, David, Henrique, Julia, Clarissa, Marcelombra e Henrique, amigos da UnB, IMPA e de Berkeley, principalmente, Malaka family: Sebastian, Marcos, Oriol, Meire, Marcelo e Ivan. Agradecimentos especias ao Dr. Kevin.

Grato pelo apoio e carinho.

Contents

List of Figures

Acknowledgments

Chapter 1

Introduction

Using Darboux's theorem, it is very easy to find Lagrangian tori inside a symplectic manifold, because any open subset of $\mathbb{C}^n$ contains many. Therefore it has been of interest in symplectic topology to understand Lagrangian submanifolds satisfying some global property, such as monotonicity (for definition of monotone Lagrangian submanifold, see section 6). On the other hand, for a long time, the only known monotone Lagrangian tori in $\mathbb{C}^n$ (up to Hamiltonian isotopy) were the products $(S^1(r))^n \subset \mathbb{C}^n$, the so called Clifford tori. Only in 1995, Chekanov introduced in his paper [5] the first examples of monotone Lagrangian tori not Hamiltonian isotopic to these.

The Clifford torus can be symplectically embedded into the complex projective space $\mathbb{CP}^n$ and the product of spheres $\times_n \mathbb{CP}^1$, giving monotone tori. Each one of these is also known as a Clifford torus. Chekanov's monotone tori were also known to give rise to exotic monotone Lagrangian tori in these spaces. But it was only much later that Chekanov and Schlenk, in [6], described in detail their family of exotic monotone Lagrangian tori in these spaces, where by exotic we mean not Hamiltonian isotopic to the Clifford torus.

In [1], Auroux studied the SYZ mirror dual (a "Landau-Ginzburg model") of a singular special Lagrangian torus fibration given on the complement of an anticanonical divisor in $\mathbb{CP}^2$. This fibration interpolates between the Clifford torus and a slightly modified version of the Chekanov torus described by Eliashberg and Polterovich in [9]. This construction explains how the count of holomorphic Maslov index 2 discs, described by the superpotential of the Landau-Ginzburg model, changes from the Clifford torus to the Chekanov torus. The key phenomenon that arises is *wall-crossing*: in the presence of the singular fiber, some other fibers bound Maslov index 0 discs. These fibers form a "wall" on the base of the fibration, separating the Clifford type torus fibers and the Chekanov type torus fibers, and accounting for differences in the count of Maslov index 2 discs between the two sides of the wall.

In this paper, we reinterpret Auroux's construction using almost toric fibrations as defined by Symington in [19]; see also [17]. The base of the relevant almost toric fibration can be represented by a *base diagram* that resembles the base of the moment map of the standard torus action on $\mathbb{CP}^2$, except that it has a marked point called *node* in the interior, representing the singular fiber, and a cut that encodes the monodromy around the singular

fiber; see Figure 1.1, where nodes are represented by ×'s and cuts by dotted lines. Modifying the almost toric fibration of a four dimensional symplectic manifold by replacing a corner (zero dimensional fiber) by a singular fiber in the interior with a cut is called *nodal trade*, also referred in this paper as 'smoothing the corner', and lengthening or shortening the cut is called *nodal slide*. Both operations are known to preserve the four-manifold up to symplectomorphism; see [17, 19].

The Clifford torus lies over the center of the standard moment map picture of $\mathbb{CP}^2$, and the small cut introduced by a nodal trade points towards it. We can lengthen the cut to pass through the Clifford torus, which develops a singularity and then becomes the Chekanov torus. This is illustrated on the first three base diagrams of Figure 1.1.

We can continue further and introduce another cut by performing a nodal trade in one of the remaining corners and lengthening it to pass by the Chekanov torus, giving rise to another monotone torus, as illustrated in Figure 1.1. This particular torus is the main focus of this paper. However, we also note that we can further perform a nodal trade on the remaining corner and pass it through the central fiber. Not only that, we can then shorten the other cuts to pass again through the central fiber, giving rise to an infinite range of monotone tori, that we conjecture not to be Hamiltonian isotopic to each other.

To perform these modifications in a more orderly way, it is convenient to redraw the almost toric base, after crossing the central fiber. This is done by fully cutting the almost toric base in two, following the considered cut, then applying the monodromy associated with the cut to one of the two components and gluing again with the other component. This move straightens the edges that intersected the original cut, while creating a new cut in the same direction as the original one but on the other side of the node. Each one of the pictures at the bottom of Figure 1.1 is related with the one right above it via this cut and glue process. Figure 2.3 illustrates more the case with only one cut: after we switch the cut to the other side, we end up with an almost toric fibration on $\mathbb{CP}^2$ with a base that resembles the polytope of the weighted projective space $\mathbb{CP}(1, 1, 4)$, but with a cut and node replacing the corner that corresponds to the orbifold singularity, and having the Chekanov torus as its central fiber. Following the isotopies generated by shortening the cut in the re-glued picture to a limit situation where the node hits the corner illustrates a degeneration of $\mathbb{CP}^2$ into $\mathbb{CP}(1, 1, 4)$.

More generally, the projective plane admits degenerations to weighted projective spaces $\mathbb{CP}(a^2, b^2, c^2)$, where (a, b, c) is a Markov triple, i. e., satisfies the Markov equation:

$$a^2 + b^2 + c^2 = 3abc.$$

All Markov triples are obtained from (1,1,1) by a sequence of 'mutations' of the form

$$(a, b, c) \rightarrow (a, b, c' = 3ab - c)$$

These degenerations of $\mathbb{CP}^2$ to other wighted projective spaces potentially give an infinite range of exotic monotone Lagrangian tori in $\mathbb{CP}^2$, since they are expected to bound different number of Maslov index 2 holomorphic discs. This was conjectured by Galkin-Usnich in
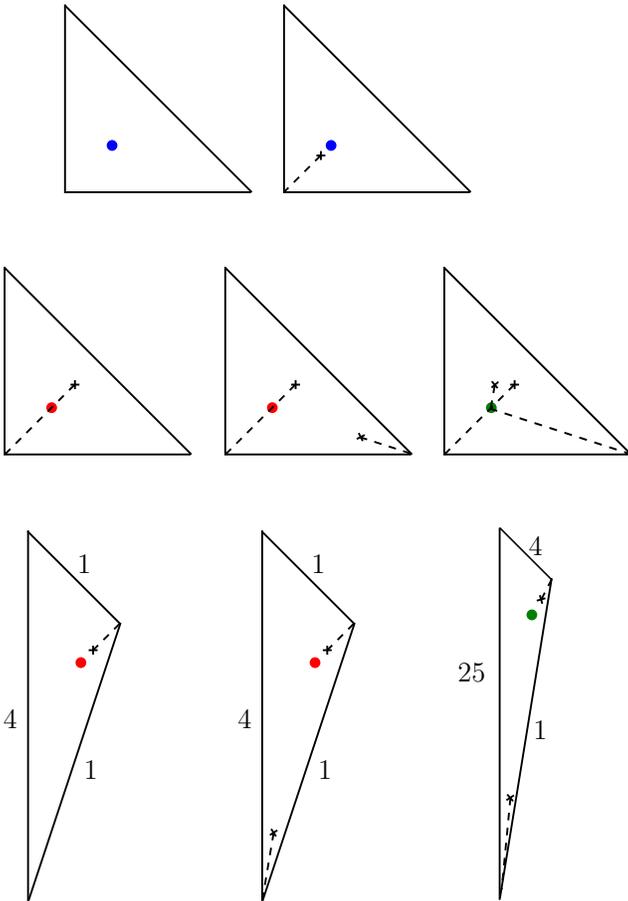
Figure 1.1: The procedure for going from the Clifford torus on the top left base diagram, to the Chekanov torus (third base diagram) and to the $T(1, 4, 25)$ torus (fifth base diagram) by applying nodal trades and nodal slides, where dots represent the image of the monotone tori in the base diagrams. Each of the bottom diagrams is equivalent to the one right above it since they are related by the cut and glue process described above and illustrated in Figure 2.3. Affine lenghts of the edges are measured relative to the respective primitive vector. For detailed explanation of pictures see section 2.3.

[11], where they also explain how to predict the superpotential related to each one of the conjectured tori by applying successive 'mutations' to the superpotential (2.4).

A degeneration from $\mathbb{CP}^2$ to $\mathbb{CP}(a^2, b^2, c^2)$ can be illustrated by almost toric pictures by introducing cuts in all corners of the standard polytope of $\mathbb{CP}^2$ via nodal trades and then performing cut and glue operations as described above, according to the sequence of mutations that links $(1, 1, 1)$ to (a, b, c). In view of this we call $B(a^2, b^2, c^2)$ the base of an almost toric fibration on $\mathbb{CP}^2$ that is about to degenerate to the toric fibration of $\mathbb{CP}(a^2, b^2, c^2)$, i.e., whose picture resembles a moment polytope of $\mathbb{CP}(a^2, b^2, c^2)$ but with

appropriate cuts, not passing through the center, joining each corner to a node. We also call $T(a^2, b^2, c^2)$ the central fiber of $B(a^2, b^2, c^2)$, so $T(1,1,1)$ is the Clifford torus and $T(1,1,4)$ is the Chekanov torus. Recalling that walls of Maslov index 0 discs divide the base of a singular Lagrangian fibration into chambers, we say that a fiber is of $T(a^2, b^2, c^2)$ type if it belongs to a chamber that (continuously deforms to a chamber that) contains the monotone $T(a^2, b^2, c^2)$ torus as a fiber, and hence bounds the same number of regular Maslov index 2 J-holomorphic discs as $T(a^2, b^2, c^2)$.

The aim of this paper is to study $T(1, 4, 25)$. First we predict the number and relative homotopy classes of regular Maslov index 2 J-holomorphic discs $T(1, 4, 25)$ bounds using wall-crossing formulas. Even though these formulas are believed to hold for the almost toric case, they are not yet completely proven rigorously, and neither is the relation between J-holomorphic discs and tropical curves upon degeneration to a 'large limit' almost complex structure.

Therefore, after that we proceed to give, purely in the language of symplectic topology, a complete self-contained proof of:

Theorem 1.0.1. *There exists a monotone Lagrangian torus in $\mathbb{CP}^2$ endowed with the standard Fubini-Study form bounding 10 families of Maslov index 2 holomorphic discs, that is not Hamiltonian isotopic to the Clifford and Chekanov tori.*

For that we modify Auroux's example described in [1], by considering a singular Lagrangian fibration that should interpolate between Chekanov type tori and $T(1, 4, 25)$ type tori.

More specifically, the rest of this paper is organized as follows.

In section 2, we review mirror symmetry in the complement of an anticanonical divisor, Landau Ginzburg models, wall-crossing phenomena and Auroux's example we mentioned above, following the approach in [1, 2].

In section 2.3, we review almost toric fibrations and in section 2.4 we explain the relationship between J-holomorphic discs and tropical discs in almost toric fibrations, working it out for the Example in section 2.1. Even though the approach is not totally rigorous, in section 3 we use tropical discs and wall-crossing formulas for an almost toric fibration to predict the existence of the $T(1, 4, 25)$ torus and the number of Maslov index 2 discs it bounds, by computing the superpotential in an informal manner.

In section 4, we use a explicit degeneration of $\mathbb{CP}^2$ into $\mathbb{CP}(1, 1, 4)$ to define $T(1, 4, 25)$ type Lagrangian tori and set the conditions for computing the Maslov index 2 holomorphic discs it bounds.

In section 5, we compute first the relative homotopy classes allowed to have Maslov index 2 holomorphic discs and then the actual Maslov index 2 holomorphic discs a $T(1, 4, 25)$ type torus bounds. We also prove regularity and orient the moduli space of holomorphic discs in each of the classes in order to determine the correct signed count for the superpotential.

In section 6, we modify the symplectic structure to construct the monotone $T(1, 4, 25)$ torus and prove that it is not symplectomorphic to the known Clifford and Chekanov tori.

Finally, in section 7, we repeat the techniques of sections 3 and 4 to conjecture the existence of an exotic monotone torus in $\mathbb{CP}^1 \times \mathbb{CP}^1$, bounding 9 families of Maslov index 2 holomorphic discs.

Chapter 2

Motivation: Mirror symmetry

This chapter is a summary of the introduction to mirror symmetry in the complement of a anti-canonical divisor explained in [1, 2]. Mirror symmetry has been extended beyond the Calabi-Yau setting by considering Landau-Ginzburg models. More precisely, it is conjectured that the Mirror of a Kähler manifold (X, ω, J), with respect to a effective anticanonical divisor D, is a Landau-Ginzburg model $(X^\vee, W)$, where $X^\vee$ is a mirror of the almost Calabi-Yau $X \backslash D$ in the SYZ sense, i.e. a (corrected and completed) moduli space of special Lagrangian tori in $X \backslash D$ equipped with rank 1 unitary local systems ($U(1)$ flat connections on the Lagrangian), and the superpotential $W : X^\vee \to \mathbb{C}$ given by Fukaya-Oh-Ohta-Ono's m_0 obstruction to Floer homology, which is a holomorphic function defined by a count of Maslov index 2 holomorphic discs with boundary on the Lagrangian; see [1,2]. Kontsevich's homological mirror symmetry conjecture predicts that the Fukaya category of X is equivalent to the derived category of singularities of the mirror Landau-Ginzburg model $(X^\vee, W)$.

In order to apply the SYZ construction to $X \backslash D$, we have to represent it as a (special) Lagrangian fibration over some base. Also, to ensure that the count of Maslov index 2 holomorphic discs is well defined, one asks L to satisfy some assumptions. More precisely, we require:

(1) there are no non-constant holomorphic discs of Maslov index 0 in (X, L);

(2) holomorphic discs of Maslov index 2 in (X, L) are regular;

(3) there are no non-constant holomorphic spheres in X with $c_1(TX) \cdot [S^2] \leq 0$.

In this case one defines the superpotential $W = m_0 : X^\vee \to \mathbb{C}$ by

Definition 2.0.2.

$$m_0(L, \nabla) = \sum_{\beta, \mu(\beta)=2} n_\beta(L) \, exp(-\int_\beta \omega) hol_\nabla(\partial \beta) \qquad (2.1)$$

where ∇ is a $U(1)$ flat connection on L, $\mathrm{hol}_\nabla(\partial\beta)$ is the holonomy around the boundary of β and $n_\beta(L)$ is the (algebraic) count of holomorphic discs in the class β whose boundary passes though a generic point $p \in L$. More precisely, considering $\mathcal{M}(L, \beta)$ the oriented (after a choice of spin structure for L) moduli space of holomorphic discs with boundary in L representing the class β, $n_\beta(L)$ is the degree of its push forward under the evaluation map at a boundary marked point as a multiple of fundamental class $[L]$, i.e., $ev_*[\mathcal{M}(L, \beta)] = n_\beta(L)[L]$.

In principle one does not know if the series (2.1) converge. Thus, it is preferable to replace the exponential by a formal parameter and the superpotential then takes values in the Novikov field. Nevertheless, all the superpotentials computed in this paper are given by a finite sums, and we use the exponential for consistency with [1].

For each $\beta \in H_2(X, L, \mathbb{Z})$, with $\partial\beta \neq 0 \in H_1(L, \mathbb{Z})$, we can define a holomorphic function $z_\beta : X^\vee \to \mathbb{C}^*$ by

$$z_\beta(L, \nabla) = \exp(-\int_\beta \omega)\mathrm{hol}_\nabla(\partial\beta); \qquad (2.2)$$

see Lemma 2.7 in [1].

Remark 2.0.3. *Actually, the function z_β is only defined locally, for we have to keep track of the relative class β under deformations of L. In the presence of non-trivial monodromy, which appears when we allow the fibration to have singular fibers, the function becomes multivalued.*

In some cases, including the Lagrangian fibrations considered in this paper, the map $H_1(L) \to H_1(X)$ induced by inclusion is trivial, and then we can get a set of holomorphic coordinates $z_j = z_{\beta_j}$ by considering relative classes β_j so that $\partial\beta_j$ forms a basis of $H_1(L)$. Then our superpotential can be written as a Laurent series in terms of such holomorphic coordinates.

In many cases we consider Lagrangian fibrations with singular fibers, and some of the Lagrangian fibers bound Maslov index 0 holomorphic discs, passing through the singular point. The projection of such Lagrangians forms "walls" in the base, dividing it into chambers. The count of Maslov index 2 holomorphic discs bounded by Lagragian fibers can vary for different chambers. This is called "wall-crossing phenomenon"; see section 2.2 and section 3 of [1]. Nevertheless, one can still construct the mirror by gluing the various chambers of the base using instanton corrections; see Proposition 3.9 and Conjecture 3.10 in [1].

The example below not only illustrates wall-crossing, but also serves as the main model for the rest of the paper. For a more detailed account, see section 5 of [1] or section 3 of [2].

2.1 A motivating example

The following example is taken from [1], section 5. We will describe it in detail because our main construction, given in section 4, can be thought as a further development of the same ideas.

Consider $\mathbb{CP}^2$, equipped with the standard Fubini-Study Kähler form, and the anticanonical divisor $D = \{(x : y : z); (xy - cz^2)z = 0\}$, for some $c \neq 0$. We will construct a family of

Lagrangian tori in the complement of the divisor D. For this we look at the pencil of conics defined by the rational map $f : (x : y : z) \mapsto (xy : z^2)$. We will mostly work with f in the affine coordinate given by $z = 1$, as a map from $\mathbb{C}^2$ to $\mathbb{C}$, $f(x, y) = xy$. The fiber of f over any non-zero complex number is then a smooth conic, while the fiber over 0 is the union of two lines, and the fiber over ∞ is a double line.

There is a S^1 action on each fiber of f given by $(x, y) \mapsto (e^{i\theta}x, e^{-i\theta}y)$. Recall that the symplectic fibration f carries a natural connection induced by the symplectic form, whose horizontal distribution is the symplectic orthogonal to the fiber. Our family of tori will consist then of parallel transports of each S^1 orbit, along circles in the base of the fibration, centered at $c \in \mathbb{C}$. We say that the height of an S^1 orbit is the value of $\mu(x, y) = \frac{1}{2}\frac{|x|^2 - |y|^2}{1 + |x|^2 + |y|^2}$, which is the negative of the moment map of the S^1 action. Let V_θ be the vector field generated by the S^1 action. Since $d\mu = -\omega(V_\theta, \cdot)$ and V_θ is contained in the tangent space of the fibers, we see that the moment map remains invariant under parallel transport. Therefore we get that our family of Lagrangian tori is given by

Definition 2.1.1. *Given $r > 0$, and a real number $\lambda \in \mathbb{R}$, set*

$$
\begin{aligned}
T_{r,\lambda}^c &= \{(x : y : z); |f(x : y : z) - c| = r; \mu(x : y : z) = \lambda\} \\
&= \{(x, y); |xy - c| = r; |x|^2 - |y|^2 = 2\lambda(1 + |x|^2 + |y|^2)\}.
\end{aligned}
\tag{2.3}
$$
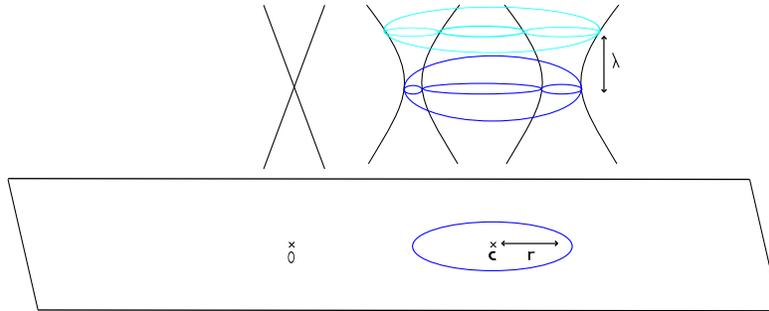
Figure 2.1: The special Lagrangian torus $T_{r,\lambda}^c$ in $\mathbb{C}^2 \setminus D$ (from [1])

Remark 2.1.2. *All the pairs consisting of a symplectic fibration together with a map from the symplectic manifold to $\mathbb{R}$ (real data) used to define the Lagrangian fibrations considered in this paper form pseudotoric structures as defined by Tyurin in [20].*

Note that actually $T_{|c|,0}^c$ is a singular torus, pinched at $(0, 0)$, so varying r and λ give us a singular toric fibration. If $r > |c|$, we say that $T_{r,\lambda}^c$ is of Clifford type, and if $r < |c|$, of Chekanov type. The motivation for this terminology is that in the first case we can deform the circle centered at c with radius r in the base to a circle centered at the origin, without crossing it, and with it we obtain a Lagrangian isotopy from $T_{r,0}^c$ to a Clifford torus

$S^1(\sqrt{r}) \times S^1(\sqrt{r})$. Not crossing the origin implies that no torus in the deformation bounds Maslov index 0 discs, hence the count of Maslov index 2 discs remains the same; see section 5.2 of [1]. On the other hand, for $r < |c|$, $T_{r,0}^c$ is the Eliashberg-Polterovich version of the so-called Chekanov torus; see [9].

To compute the Maslov index of discs in terms of their algebraic intersection number with the divisor D, one can prove that these Lagrangian tori are special with respect to the holomorphic 2-form $\Omega(x,y) = (xy - c)^{-1}dx \wedge dy$. In general, we can associate to an anticanonical divisor D a nonvanishing holomorphic n-form Ω on the complement $X \setminus D$ given by the inverse of a section of the anticanonical bundle that defines D. Recall the following definition:

Definition 2.1.3. *A Lagrangian submanifold L is said to be special Lagrangian, with respect to Ω and with phase ϕ, if $Im(e^{-i\phi}\Omega)_{|L} = 0$.*

For a proof that $T_{r,\lambda}^c$ are special Lagrangian with respect to Ω, see proposition 5.2 of [1]. The following is Lemma 3.1 of [1].

Lemma 2.1.4. *If $L \subset X \setminus D$ is special Lagrangian, then for any relative homotopy class $\beta \in \pi_2(X, L)$ the Maslov index of β, $\mu(\beta)$, is equal to twice the algebraic intersection number $\beta \cdot [D]$.*

It can also be shown that $T_{r,\lambda}^c$ bounds Maslov index 0 holomorphic discs if and only if $r = |c|$. So we see that $r = |c|$ creates a wall in the base of our Lagrangian fibration given by pairs (r, λ). Then we need to treat the cases $r > |c|$ and $r < |c|$ separately.

For $r > |c|$, we argue that $T_{r,\lambda}^c$ is Lagrangian isotopic to a product torus $S^1(r_1) \times S^1(r_2)$, without altering the disc count throughout the deformation. Denote by z_1 and z_2 respectively the holomorphic coordinates on the mirror associated to the relative homotopy classes β_1 and β_2 of discs parallel to the x and y coordinate axes in $(\mathbb{C}^2, S^1(r_1) \times S^1(r_2))$. Namely, $z_i = \exp(-\int_{\beta_i} \omega)\text{hol}_\nabla(\partial\beta_i)$. We get from Proposition 4.3 of [1] that the superpotential recording the counts of Maslov index 2 holomorphic discs bounded by $T_{r,\lambda}^c$ for $r > |c|$ is given by

$$W = z_1 + z_2 + \frac{e^{-\Lambda}}{z_1 z_2}, \tag{2.4}$$

where $\Lambda = \int_{[\mathbb{CP}^1]} \omega$. The term $\frac{e^{-\Lambda}}{z_1 z_2}$ corresponds to discs that project via f to a double cover of $\mathbb{C}^2 \setminus \Delta$ branched at infinity lying in the class $[\mathbb{CP}^1] - \beta_1 - \beta_2 \in \pi_2(\mathbb{CP}^2, T_{r,0}^c)$. The other terms z_1 and z_2 of the superpotential correspond to sections of f over the disc Δ centered at c with radius r, intersecting respectively the components $\{x = 0\}$ and $\{y = 0\}$ of the fiber $f^{-1}(0)$.

Now we look at the case $r < |c|$, and consider the special case $\lambda = 0$, the Chekanov torus considered by Eliashberg-Polterovich in [9]. One family of Maslov index 2 holomorphic discs lies over the disc Δ centered at c with radius r, given by the intersection of $f^{-1}(\Delta)$ with the lines $x = e^{i\theta}y$. We denote by β their relative class in $\pi_2(\mathbb{CP}^2, T_{r,0}^c)$. The other discs

are harder to construct. Consider the class α of the Lefschetz thimble associated with the critical point of f at the origin and the vanishing path $[0, c - re^{\arg(c)i}]$. One can see that α, β and $H = [\mathbb{CP}^1]$ form a basis of $\pi_2(\mathbb{CP}^2, T_{r,0}^c)$. The following Lemma and Proposition, due to Chekanov-Schlenk [6], have their proofs sketched in [1].

Lemma 2.1.5 (Chekanov-Schlenk [6]). *The only classes in $\pi_2(\mathbb{CP}^2, T_{r,0}^c)$ which may contain Maslov index 2 holomorphic discs are β and $H - 2\beta + k\alpha$ for $k \in \{-1, 0, 1\}$.*

Proposition 2.1.6 (Chekanov-Schlenk [6]). *The torus $T_{r,0}^c$ bounds a unique S^1 family of holomorphic discs in each of the classes β and $H - 2\beta + k\alpha$ for $k \in \{-1, 0, 1\}$. These discs are regular, and the corresponding algebraic count is 2 for $H - 2\beta$ and 1 for the other classes.*

Since deforming λ to 0 yields a Lagrangian isotopy from $T_{r,\lambda}^c$ to $T_{r,0}^c$ in the complement of $f^{-1}(0)$, so without encountering any Maslov index 0 holomorphic discs, the disc count remains the same and we have that for $r < |c|$ the superpotential is given by

$$W = u + \frac{e^{-\Lambda}}{u^2 w} + 2\frac{e^{-\Lambda}}{u^2} + \frac{e^{-\Lambda} w}{u^2} = u + \frac{e^{-\Lambda}(1 + w)^2}{wu^2} \tag{2.5}$$

where u and w are the holomorphic coordinates on the mirror associated to the class β and α.
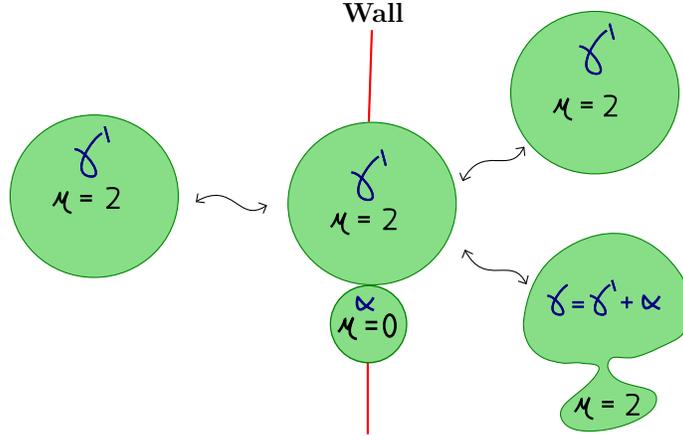
Figure 2.2: Wall-crossing: Following a Maslov index 2 holomorphic disc through a Lagrangian deformation of the fibers crossing a wall consisting of fibers bounding Maslov index 0 discs (see Figure 2.7 for the tropical picture).

2.2 Wall-crossing

In this section we explain the wall-crossing phenomenon. Then we see how it happens in Example 2.1 and explain the relation between the two formulas for the superpotential in terms of the wall-crossing at $r = |c|$, still following section 5 of [1].

Let us follow a Maslov index 2 holomorphic disc in a class γ' through a Lagrangian deformation of the fibers crossing a wall (formed by projection of fibers bounding Maslov index 0 discs). Assume that the given disc continues to exist throughout the deformation. The following phenomenon typically happens: if the boundary of such a disc intersects that of a Maslov index 0 holomorphic disc in a class α while on the wall, they can be glued into another Maslov index 2 disc, in the class $\gamma = \gamma' + \alpha$, on the other side of the wall, besides the deformation that passes through, in the "same" class γ', without attaching the Maslov index 0 disc. Conversely, a Maslov index 2 holomorphic disc in a class γ can split into a Maslov index 2 holomorphic disc in a class γ' and a Maslov index 0 holomorphic disc in a class γ, while on the wall, and then disappear after the Lagrangian passes through; see Figure 2.2.

We see how this phenomenon appears in the Example 2.1. Begin considering the case where $\lambda > 0$, so $T_{r,\lambda}^c$ lies in the region where $|x| > |y|$. Then when $r = |c|$ the torus intersects $\{y = 0\}$ in a circle bounding a Maslov index 0 disc, u_0. This disc represents the class α, on the Chekanov side, and $\beta_1 - \beta_2$, on the Clifford side. As r decreases through $|c|$, the family of holomorphic discs in the class β_2 on the Clifford side become the family of discs on the class β on the Chekanov side, and the discs in the class $H - \beta_1 - \beta_2$ on the Clifford side becomes the discs in the class $H - 2\beta - \alpha$ on the Chekanov side.

Since a disc in the class $H - 2\beta - \alpha$, bounded by a torus over the wall $r = |c|$, intersects u_0 in $[H - 2\beta - \alpha] \cdot [\alpha] = 2$ points, new discs in the classes $H - 2\beta$ and $H - 2\beta + \alpha$ arise from attaching u_0 to a disc in the class $H - \beta_1 - \beta_2 = H - 2\beta - \alpha$ at one or both points where their boundaries intersect. On the other hand, a discs in the class β, at the wall, intersects the Maslov index 0 disc u_0 at one point. When crossed to the Clifford side, a disc in the class $\beta_1 = \beta_2 + \alpha$ arrises from attaching u_0 to a disc in the class $\beta_2 = \beta$; see Figures 2.5, 2.6, 2.7 (in these figures, discs are represented tropically). Conversely, one can think that a holomorphic disc in the class β_1 on the Clifford side, when deformed towards the wall, breaks into a holomorphic disc in the class $\beta = \beta_1 - \alpha$ and the Maslov index 0 disc u_0 and then disappears on the Chekanov side.

For $\lambda < 0$, when $r = |c|$ the torus intersects $\{x = 0\}$ in a circle bounding a Maslov index 0 disc in the class $\beta_2 - \beta_1 = -\alpha$. As r decreases through $|c|$, the families of holomorphic discs that survive the deformation through the wall are in the classes β_2 and $H - \beta_1 - \beta_2$ on the Clifford side, becoming β and $H - 2\beta - \alpha$ on the Chekanov side. As before, two new families of discs are created in the classes $H - 2\beta$ and $H - 2\beta + \alpha$, while discs in the classes β_1 disappear, after wall-crossing.

The difference between the "naive" gluing formulas, which for $\lambda > 0$ matches $\beta \leftrightarrows \beta_2$ and for $\lambda < 0$ matches $\beta \leftrightarrows \beta_1$, is due to the monodromy of the Lagrangian fibers $T_{r,\lambda}^c$ around the nodal fiber $T_{|c|,0}^c$, which is explained in the next section. However, one can perform wall-crossing corrections to take care of this discrepancy and yield a single consistent gluing for

both halves of the wall.

A holomorphic disc in the class β on the Chekanov side is thought to correspond to both discs in the classes β_1 and β_2, taking into account the attachment of the holomorphic disc u_0 in the class α. In terms of the coordinates z_1, z_2 on the Clifford side, associated with β_1 and β_2, and coordinates u and w on the Chekanov side, associated with β and α, the gluing becomes $u \leftrightarrows z_1 + z_2$.

For $\lambda > 0$, one can think that the "naive" formula $u = z_2$ is modified by a multiplicative factor of $1 + w$, i. e. , $u = (1 + w)z_2 = z_1 + z_2$, as predicted in Proposition 3.9 of [1]. For $\lambda < 0$, the correct change of coordinates is $u = z_1(1 + w^{-1}) = z_1 + z_2$, $w^{-1} = z_2/z_1$, which is the same as for $\lambda > 0$.

Taking the wall-crossing into account the correct change of coordinates in the mirror is given as follows:

Homology Classes	Coordinates
$\alpha \leftrightarrows \beta_1 - \beta_2$	$w \leftrightarrows \frac{z_1}{z_2}$
$\beta \leftrightarrows \{\beta_1, \beta_2\}$	$u \leftrightarrows z_1 + z_2$
$H - 2\beta + \{-1, 0, 1\}\alpha \leftrightarrows H - \beta_1 - \beta_2$	$\frac{e^{-\Lambda}(1+w)^2}{u^2 w} \leftrightarrows \frac{e^{-\Lambda}}{z_1 z_2}$

It is then easy to check that the formulas (2.4) and (2.5) for the superpotential, and this corrected coordinate change, do match up.

2.3 Almost toric manifolds

The aim of this section is to explain the geometry of almost toric fibrations and use it for a better understanding of the singular Lagrangian fibration in the previous example. Most importantly, we can use it to construct other fibrations and predict the superpotential on each of the chambers divided by the walls. This way we can predict existence of exotic Lagrangian tori in almost toric manifolds, and in particular the torus in $\mathbb{CP}^2$ that appears in Theorem 1.0.1. For a more detailed explanation of almost toric fibrations, see [17, 19].

The following is definition 2.2 of [17]:

Definition 2.3.1. *An* almost toric fibration *of a symplectic four manifold* (M, ω) *is a Lagrangian fibration* $\pi : (M, \omega) \to B$ *such that any point of* (M, ω) *has a Darboux neighborhood (with symplectic form* $dx_1 \wedge dy_1 + dx_2 \wedge dy_2$*) in which the map* π *has one of the following forms:*

$$
\begin{aligned}
\pi(x,y) &= (x_1, x_2), & \text{regular point,} \\
\pi(x,y) &= (x_1, x_2^2 + y_2^2), & \text{elliptic, corank one,} \\
\pi(x,y) &= (x_1^2 + x_2^2, x_2^2 + y_2^2), & \text{elliptic, corank two,} \\
\pi(x,y) &= (x_1 y_1 + x_2 y_2, x_1 y_2 - x_2 y_1), & \text{nodal or focus-focus,}
\end{aligned}
$$

with respect to some choice of coordinates near the image point in B. An almost toric manifold *is a symplectic manifold equipped with an almost toric fibration. A* toric fibration *is a Lagrangian fibration induced by an effective Hamiltonian torus action.*

We call the image of each nodal singularity a *node*.

Recall that a Lagrangian fibration yields an integral affine structure, called symplectic, on the complement of the singular values on the base, i.e. each tangent space contains a distinguished lattice. These lattices are defined in terms of the isotropy subgroups of a natural action of T^*B on M given by the time-one flow of a vector field associated with each covector of T^*B. More precisely, take $\xi \in T^*B$ and consider the vector field V_ξ defined by $\omega(., V_\xi) = \pi^*\xi$. Set $\xi \cdot x = \phi_\xi(x)$, where ϕ_ξ is the time-one flow of V_ξ. Call Λ^* the isotropy subgroup of the action, which is a lattice such that $(T^*B/\Lambda^*, d\alpha_{can})$ and (M, ω) are locally fiberwise symplectomorphic (here, α_{can} is induced by the canonical 1-form of T^*B). This induces two other lattices, the dual lattice, Λ given by $\Lambda_b = \{u \in T_b B \; ; \; v^*u \in \mathbb{Z}, \forall \, v^* \in \Lambda_b^*\}$, inside TB, and the vertical lattice, $\Lambda^{vert} = \{V_\xi \; ; \; \xi \in \Lambda^*\}$, inside the vertical bundle in TM. We call the pair (B, Λ) a *almost toric base*.

For an almost toric four manifold, the affine structure defined by the lattice above, completely determines M up to symplectomorphism, at least when the base is either non-compact or compact with non-empty boundary; see Corollary 5.4 in [19]. Also, since $(T^*B/\Lambda^*, d\alpha_{can})$ and (M, ω) are locally fiberwise symplectomorphic, a basis of the lattice is in correspondence with a basis of the first homology of the fiber over a regular point, $H_1(F_b)$. Therefore, the topological monodromy around each node is equivalent to the integral affine monodromy. The neighborhood of a nodal fiber is symplectomorphic to a standard model (see section 4.2 in [19]) and the monodromy around a singular fiber (of rank 1) is given by a Dehn twist. In suitable coordinates the Dehn twist can be represented by the matrix :

$$
A_{(1,0)} = \begin{pmatrix} 1 & 1 \\ 0 & 1 \end{pmatrix}
$$

A change of basis of $H_1(F_b)$ gives a conjugate of $A_{(1,0)}$, which is, in terms of its eigenvector (a, b):

$$
A_{(a,b)} = \begin{pmatrix} 1 - ab & a^2 \\ -b^2 & 1 + ab \end{pmatrix}
$$

Due to the monodromy, one cannot find an affine embedding of the base of an almost toric fibration with nodes into $\mathbb{R}^2$ equipped with its standard affine structure Λ_0. However,

after removing a set of *branch curves* in the base B, i.e., a collection of disjoint properly embedded curves connecting each node to a point in $\partial \bar{B}$, it may be possible to define such an embedding.
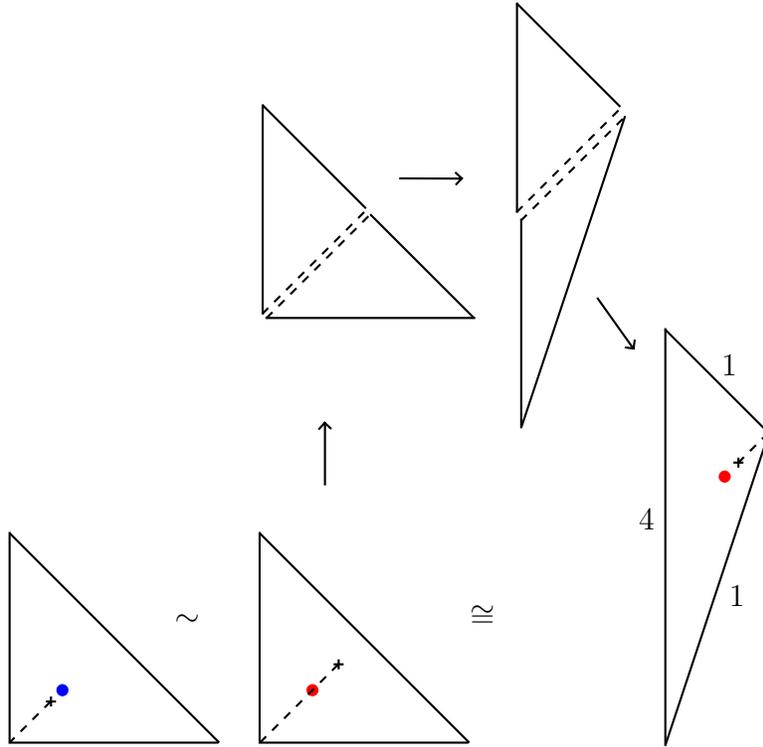
Figure 2.3: The leftmost picture is a base diagram of the almost toric fibration of $\mathbb{CP}^2$ related to the singular Lagrangian fibration given in Example 2.1 (for small c), having the Clifford torus as its central fiber. The next base diagram is obtained by applying a nodal slide passing through the Clifford torus, so that the central fiber becomes the Chekanov torus. Following the arrows we first cut the previous picture in the direction of $(1, 1)$, then we apply the monodromy $A_{(1,1)}$ to the bottom part and finally we re-glue the parts to obtain a base diagram representing the same almost toric fibration.

Definition 2.3.2 (3.2 of [17]). *Suppose we have an integral affine embedding $\Phi : (B-R, \Lambda) \to (\mathbb{R}^2, \Lambda_0)$, where (B, Λ) is an almost toric base and R is a set of branch curves. A base diagram of (B, Λ) with respect to R and Φ is the image of Φ decorated with the following data:*

- *an* x *marking the location of each node and*

- *dashed lines indicating the portion of $\partial\overline{\Phi(B-R)}$ that corresponds to R.*

Remark 2.3.3. *The presence of monodromy in the affine structure on B implies the existence of monodromy in the affine structure induced on the mirror $X^\vee$. This explains the discrepancy between the uncorrected coordinate changes across the two halves of the wall in Example 2.1. See remark 5.11 in [1].*

The affine direction(s) of the image of such a branch curve in $\mathbb{R}^2$ determine the monodromy around the corresponding node. If the image is contained in a line with direction (a, b), the monodromy is given by $A_{(a,b)}$; for a more detailed account of base diagrams, see section 5.2 of [19]. For instance, the leftmost picture of Figure 2.3 represents the Lagrangian fibration seen in Example 2.1. The ray represented by dashed lines in the direction $(1, 1)$ is an eigenvector of the monodromy, which hence is given by $A_{(1,1)}$.

Two almost toric surgery operations are of importance for us. They change the almost toric fibration into another almost toric fibration of the same symplectic four manifold and are defined as follows:

Definition 2.3.4 (4.1 of [17]). *Let (B, Λ_i) be two almost toric bases, $i = 1, 2$. We say that (B, Λ_1) and (B, Λ_2) are related by a* nodal slide *if there is a curve γ in B such that*

- *$(B - \gamma, \Lambda_1)$ and $(B - \gamma, \Lambda_2)$ are isomorphic,*

- *γ contains one node of (B, Λ_i) for each i and*

- *γ is contained in the eigenline (line preserved by the monodromy) through that node.*

Definition 2.3.5 (4.2 of [17]). *Let (B_i, Λ_i) be two almost toric bases, $i = 1, 2$. We say that (B_1, Λ_1) and (B_2, Λ_2) differ by a* nodal trade *if each contains a curve γ_i starting at ∂B_i such that $(B_1 - \gamma_1, \Lambda_1)$ and $(B_2 - \gamma_2, \Lambda_2)$ are isomorphic, and (B_1, Λ_1) has one less vertex than (B_2, Λ_2).*

Remark 2.3.6. *The rightmost picture of Figure 2.3 is not considered to differ by a nodal trade from the moment polytope of $\mathbb{CP}(1, 1, 4)$, because the latter, being the base of an* orbifold *toric Lagrangian fibration, is not considered to be an almost toric base.*

In Figure 2.3, the leftmost base diagram is obtained by applying a nodal trade to a corner of the moment polytope of $\mathbb{CP}^2$, which is the base diagram for the standard toric fibration of $\mathbb{CP}^2$. The following picture is then obtained by a nodal slide. As explained in the introduction, once the singular fiber passes trough the Clifford torus, the central fiber develops a singularity and then becomes the Chekanov torus. The rightmost picture is a $B(1, 1, 4)$ base diagram representing the same almost toric fibration. Shortening the cut to a limit situation where it hits the corner describes a degeneration of $\mathbb{CP}^2$ into $\mathbb{CP}(1, 1, 4)$.

2.4 Holomorphic discs viewed from almost toric fibrations and wall-crossing

In this section we use almost toric pictures to describe a limit affine structure of the fibration for which holomorphic curves converge to tropical curves. We illustrate the Maslov index 2 tropical discs given in this limit affine structure for the almost toric fibration considered of Example 2.1. This section is not intended to contain a rigorous approach to the correspondence between tropical curves and holomorphic discs in an almost toric setting.

Assume one has an almost toric fibration with special Lagrangian fibers with respect to Ω, a holomorphic 2-form with poles on the divisor D that projects to the boundary of the base B. Then the interior of B carries a second affine structure, sometimes called complex. The lattice which describes this affine structure, which we denote by Λ^c, is given by identifying $T_b B \simeq H^1(L_b, \mathbb{R})$, via the flux of the imaginary part of Ω and via Poincarè duality with $H_1(L_b, \mathbb{R}) \supset H_1(L_b, \mathbb{Z})$. More precisely, for each vector $v \in T_b B$ one gets the element of $H^1(L_b, \mathbb{R})$ given by the homomorphism

$$[\gamma] \in H_1(L_b, \mathbb{R}) \mapsto \left. \frac{d}{dt} \right|_{t=0} \int_{\Gamma_t} Im(\Omega),$$

where Γ_t is given by any parallel transport of γ over a curve $c(t)$ on the base, with $c(0) = b$, $c'(0) = v$. Since $Im(\Omega)$ is a closed form, vanishing on the fibers, the above is independent of $c(t)$ and Γ_t, and hence well defined. A fiber over the boundary of B is infinitely far from a given fiber over an interior point, since Ω has a pole on the divisor D.
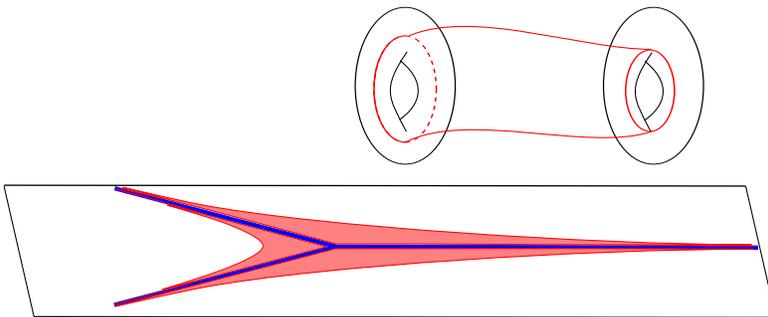
Figure 2.4: After a deformation of the almost complex structure, J-holomorphic discs project to amoebas eventually converging to tropical curves in the large complex structure limit.

In general, the projections to B of holomorphic curves, called amoebas, can be fairly complicated. However, it is expected that under a suitable deformation of the almost complex structure J towards a 'large limit' (where the base directions are stretched), the amoebas converge to tropical curves; see Figure 2.4. Also, the wall generated by the singular fiber converges to a straight line with respect to this affine structure, since it is the projection of a

holomorphic curve containing Maslov index zero discs bounded by the fibers. Moreover, since the boundary of such a disc represents the vanishing cycle in the neighborhood of the nodal fiber, its homology class is fixed by the monodromy. Hence the straight line corresponding to the wall is in the direction of the eigenvector of the affine monodromy. In a neighborhood of a fiber away from the singular ones the almost toric fibration are expected to approach $TB/\epsilon\Lambda^c$ with $\epsilon \to 0$ at the limit. This way, the change of coordinates and monodromy for this 'large limit' complex affine structure is given by the transpose inverse of the symplectic affine structure defined in section 2.3, where the neighborhood of a regular fiber is isomorphic to a neighborhood of T^*B/Λ^*. Also, our 'limit lattice' at a point b on the base is identified with $H_1(L_b, \mathbb{Z})$.

This principle is illustrated for Example 2.1 in Figures 2.5 and 2.6. In these two figures:

- The Lagrangian torus under consideration is the fiber over the thick point.

- The dashed lines represent the walls (long dashes) and the cuts (short dashes), and 'x' represents the node (singular fiber).

- A *tropical disc* is a tree whose edges are straight lines with rational slope in B, starting at the torus and ending on the nodes or perpendicular to the boundary at infinity. The internal vertices satisfy the balancing condition that the primitive integer vectors entering each vertex of the tree, counted with multiplicity, must sum to 0.

- The Maslov index of the disc equals twice the number of intersection with the boundary at infinity, i.e., the divisor.

- The multiplicity of each edge is depicted by the numbers of lines on Figure 2.6, but on some other figures the multiplicities are represented by the thickness of the line, for visual purposes (they can be computed taking into account the balancing condition).

- The vanishing cycle is represented by $(-1, 1)$ on the lattice $H_1(L_b, \mathbb{Z})$.

The relation between these pictures and the formulas in section 2.1 is as follows: z_1, z_2 are coordinates on the Clifford side associated with the vectors $(1, 0)$ and $(0, 1)$, respectively, and u, w are coordinates on the Chekanov side associated with the vectors $(1, 0)$ and $(-1, 1)$, respectively, for the top part of the Chekanov side (when $\lambda < 0$). The direction of the edge leaving the torus can be read off from the superpotential and is the negative of the vector representing the exponents of the corresponding monomial. For instance, the disc associated with the monomial $\frac{e^{-\Lambda}}{z_1 z_2}$ in (2.4) leaves the torus with tangent vector $(1, 1)$ in Figure 2.5, while the disc associated with the term $\frac{e^{-\Lambda}}{u^2}$ in (2.5) has tangent vector $(2, 0)$ (multiplicity 2) in Figure 2.6. We call this vector the "class" of the tropical disc.

The formulas for the two superpotentials are related by a *wall-crossing transformation* (or *mutation*). We describe it now for the case of a two dimensional base. In what follows, when referring to a particular fiber L_b, let β_1, β_2 be relative homotopy classes of discs with boundary on L_b such that $\partial\beta_1$, $\partial\beta_2$ are associated with $(1, 0)$ and $(0, 1)$ seen as elements of
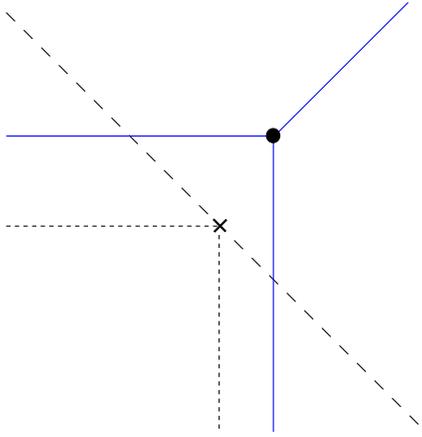
Figure 2.5: Clifford type torus. $W = z_1 + z_2 + \frac{e^{-\Lambda}}{z_1 z_2}$.
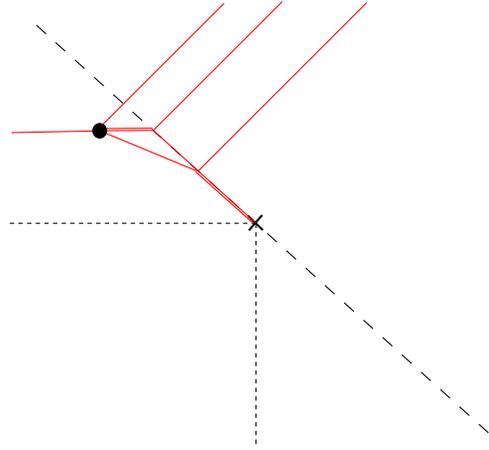
Figure 2.6: Chekanov type torus. $W = u + \frac{e^{-\Lambda}}{u^2 w} + 2\frac{e^{-\Lambda}}{u^2} + \frac{e^{-\Lambda} w}{u^2} = u + \frac{e^{-\Lambda}(1+w)^2}{u^2}$.
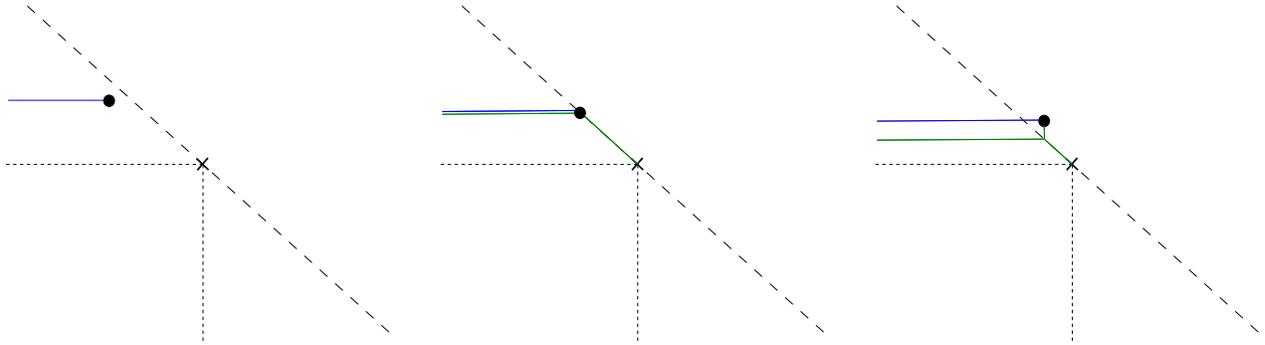
Figure 2.7: As in Example 2.1 (see also Figure 2.2), a disc in the class β_2 breaks into a disc in the class β_1 and the exceptional disc u_0, and disappears after crossing the wall, for $\lambda < 0$.

$H_1(L_b, \mathbb{Z})$, respectively. Moving the point b on the base, we keep denoting by β_1, β_2 the continuous deformations of this relative classes. Consider a wall in B coming from the projection of a family of Maslov index zero discs propagating out of a node in the base along the affine direction $(m, n) \in \mathbb{Z}^2$. (Here we only consider the part of the wall that lies on the positive half of the eigenline generated by (m, n)). Set $\mathcal{W}^+ = \{v \in \mathbb{R}^2 | \{v, (m, n)\}$ is positively oriented$\}$ and $\mathcal{W}^- = \{v \in \mathbb{R}^2 | \{v, (m, n)\}$ is negatively oriented$\}$. Denote by z_1, z_2 (respectively u_1, u_2), the coordinates associated with β_1, β_2 for the fibers L_b with b in the chamber contained in $\mathcal{W}^+$ (respectively $\mathcal{W}^-$). The class of the primitive Maslov index zero discs bounded by the fibers along the wall is of the form $m\beta_1 + n\beta_2 + k[\mathbb{CP}^1]$ and hence is represented by the monomial $w = e^{-k\Lambda} z_1^m z_2^n = e^{-k\Lambda} u_1^m u_2^n$. The coordinates z_1, z_2 and u_1, u_2 are then related by the:

Wall-crossing formula

$$u_1^r u_2^s \rightleftharpoons z_1^r z_2^s (1 + w)^{nr - ms} \tag{2.6}$$

That way, knowing the superpotential on one side of the wall, it is expected that one can compute the superpotential of the other side by applying the above wall-crossing formula. Note that the absolute value of the exponent $|nr - ms|$ is the intersection number between a disc represented by $z_1^r z_2^s$ and the Maslov index zero disc at a fiber over the wall.

Chapter 3

Predicting the enumerative geometry of $T(1, 4, 25)$

In this chapter we apply the same ideas as in the previous section to another almost toric fibration, any of the ones shown on Figure 3.1, to predict the superpotential of the $T(1, 4, 25)$ *type* torus, obtained from the previous Chekanov torus after another wall-crossing.

Figure 3.1 represents almost toric fibrations on $\mathbb{CP}^2$ containing two singular fibers of rank one. The middle diagram arises by applying a nodal trade to one corner of the right-most diagram in Figure 2.3, after redrawing the diagram via an element of $AGL(2, \mathbb{Z})$, which is, up to translation, $\begin{pmatrix} 1 & 0 \\ -3 & 1 \end{pmatrix}$. Lengthening the new cut to pass trough the central fiber we end up with an almost toric fibration having the monotone $T(1, 4, 25)$ torus as a fiber, as illustrated by the right-most diagram in Figure 3.1.

We assume the Lagrangian fibers are special with respect to some 2-form Ω with poles on the divisor, and that in a 'large limit' almost complex structure, pseudo-holomorphic curves project to tropical curves. We will start the description of the superpotential in the chambers where the fibers are of Clifford type and successively cross two walls in order to arrive at a tentative formula for the superpotential in the chamber where the fibers are $T(1, 4, 25)$ type tori. In section 4, we construct a singular Lagrangian fibration interpolating between Chekanov type tori and $T(1, 4, 25)$ type tori. For the later, the count of Maslov index 2 holomorphic discs is verified rigorously in section 5 using only symplectic geometry techniques.

Now we focus on the chamber containing the Clifford type tori illustrated on the top right part of Figure 3.2. Since we applied $\begin{pmatrix} 1 & 0 \\ -3 & 1 \end{pmatrix}$ to the right-most diagram of Figure 2.3, we need to 'dually' change the coordinates used on Figure 2.5 by applying the transpose inverse $\begin{pmatrix} 1 & 3 \\ 0 & 1 \end{pmatrix}$. Calling these new coordinates $\hat{z}_1$, $\hat{z}_2$, associated with $(1, 0)$ and $(0, 1)$ on the top right part of Figure 3.2, they are described in terms of z_1, z_2 by $z_1 = \hat{z}_1$, $z_2 = \hat{z}_1^3 \hat{z}_2$. This way a tropical disc in the class (p, q) on the top right part of Figure 3.2 corresponds to
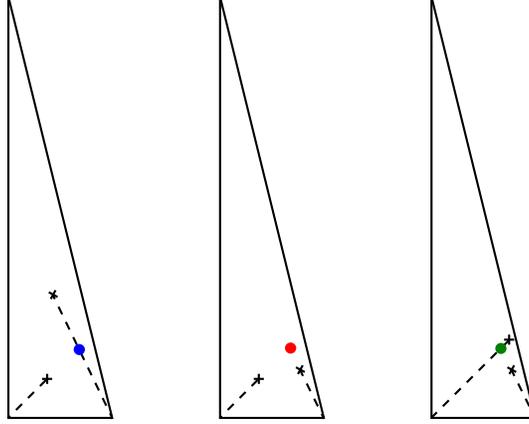
Figure 3.1: Almost toric base diagrams of $\mathbb{CP}^2$ having, respectively, the monotone Clifford, Chekanov and $T(1,4,25)$ tori as the a fiber.

a monomial with exponents $\hat{z}_1^p \hat{z}_2^q$. After this change of coordinates, the invariant direction at the singularity is $(2,1)$ and the monodromy is given by $A_{(2,1)}$; see Figure 3.2. Therefore at the top part of the chamber corresponding to the Clifford type tori the superpotential is given by

$$W_{Clif} = \hat{z}_1 + \hat{z}_1^3 \hat{z}_2 + \frac{e^{-\Lambda}}{\hat{z}_1^4 z_2} \tag{3.1}$$

As the vanishing vector of the first wall is $(2,1)$, the vanishing class is represented by the coordinate $\tilde{w} = \hat{z}_1^2 \hat{z}_2 = \tilde{z}_1^2 \tilde{z}_2$, where $\tilde{z}_1$, $\tilde{z}_2$ are the coordinates corresponding to the standard basis on the Chekanov side. Applying the wall crossing formula 2.6 to (3.1), the superpotential in the Chekanov region is

$$W_{Che} = \tilde{z}_1 + e^{-\Lambda} \frac{(1 + \tilde{w})^2}{\tilde{z}_1^4 \tilde{z}_2} = \tilde{z}_1 + e^{-\Lambda} \tilde{z}_2 + 2 \frac{e^{-\Lambda}}{\tilde{z}_1^2} + \frac{e^{-\Lambda}}{\tilde{z}_1^4 \tilde{z}_2}. \tag{3.2}$$

We now cross the second wall towards a $T(1,4,25)$ type torus. The second wall has vanishing vector $(-1,1)$ and the monomial corresponding to the vanishing class is $w = e^{-\Lambda} \tilde{z}_2 \tilde{z}_1^{-1} = e^{-\Lambda} u_2 u_1^{-1}$, where u_1, u_2 are are the coordinates corresponding to the standard basis on the $T(1,4,25)$ side and the factor $e^{-\Lambda}$ is present because the class of the Maslov index 0 disc is $-\beta_1 + \beta_2 + [\mathbb{CP}^1] \in \pi_2(\mathbb{CP}^2, L)$, where β_1 and β_2 are the classes associated with the coordinates, $\tilde{z}_1$, $\tilde{z}_2$. Indeed, knowing the boundary of w represents the class $(-1,1)$, we get the first two coefficients of β_1 and β_2. To obtain the coefficient of $[\mathbb{CP}^1]$ we compute the Maslov index. We have that $\mu([\mathbb{CP}^1]) = 6$ (see Lemma 2.1.4) and $\tilde{z}_1$ and $e^{-\Lambda} \tilde{z}_2$ are terms in W_{Che}, hence $\mu(\beta_1) = 2$ and $\mu(\beta_2) = -4$. In order to have Maslov index 0, the coefficient of $[\mathbb{CP}^1]$ must be 1. Finally, applying the wall-crossing formula 2.6 to (3.2) we get that
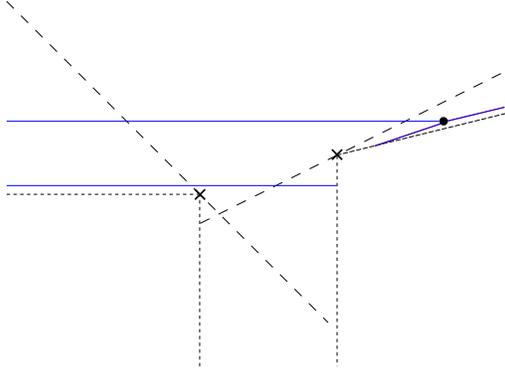
Figure 3.2: Clifford type torus. $W_{Clif} = \hat{z}_1 + \hat{z}_1^3 \hat{z}_2 + \frac{e^{-\Lambda}}{\hat{z}_1^4 z_2}$.
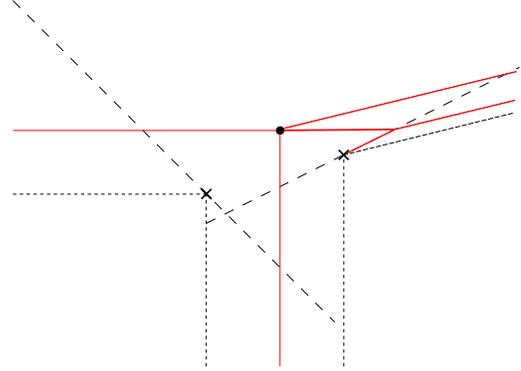
Figure 3.3: Chekanov type torus. $W_{Che} = \tilde{z}_1 + e^{-\Lambda} \tilde{z}_2 + 2\frac{e^{-\Lambda}}{\tilde{z}_1^2} + \frac{e^{-\Lambda}}{\tilde{z}_1^4 \tilde{z}_2}$.

$$
\begin{aligned}
W_{T(1,4,25)} &= u_1 + 2\frac{e^{-\Lambda}}{u_1^2}(1+w)^2 + \frac{e^{-\Lambda}}{u_1^4 u_2}(1+w)^5 \\
&= u_1 + 2\frac{e^{-\Lambda}}{u_1^2} + 4\frac{e^{-\Lambda}u_2}{u_1^3} + 2\frac{e^{-\Lambda}u_2^2}{u_1^4} + \frac{e^{-\Lambda}}{u_1^4 u_2} + 5\frac{e^{-2\Lambda}}{u_1^5} \\
&\quad + 10\frac{e^{-3\Lambda}u_2}{u_1^6} + 10\frac{e^{-4\Lambda}u_2^2}{u_1^7} + 5\frac{e^{-5\Lambda}u_2^3}{u_1^8} + \frac{e^{-6\Lambda}u_2^4}{u_1^9} \\
&= u + 2\frac{e^{-\Lambda}}{u^2}(1+w)^2 + \frac{e^{-2\Lambda}}{u^5 w}(1+w)^5. \qquad (3.3)
\end{aligned}
$$

The last formula is a more simplified expression in terms of the coordinates $u = u_1$ and w. The expanded version in coordinates u_1, u_2 makes it easier to visualize the class of each disc. Figure 3.4 illustrates a $T(1, 4, 25)$ type torus, predicted to bound 10 different families of holomorphic discs, corresponding to the 10 terms in this expression.

Even though our approach in this section was not completely rigorous, it points toward the existence of such an exotic torus bounding 41 discs, if we count with multiplicity (sum the coefficients of each monomial). The theory for proving the correspondence between tropical curves on the base and holomorphic curves on the total space is not fully developed yet, so the actual proof in section 5 will use a different approach.

Remark 3.0.1. *The bottom most region on Figures 3.2-3.4 is known to have infinitely many walls, since it can have Maslov index 0 discs ending in both nodes with different multiplicities. This can be detected by the need for consistency of the changes of coordinates due to wall-crossing when we go around the point where the walls intersect. This phenomenon is called scattering, first described by M. Kontsevich and Y.Soibelman in [14]. See also M. Gross [12].*
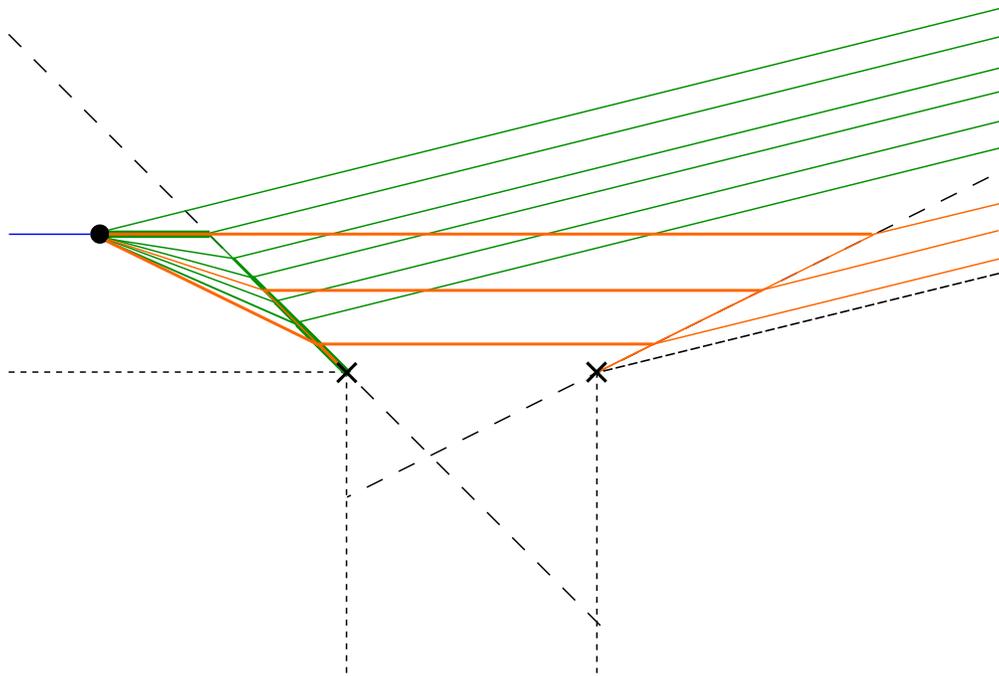
Figure 3.4: A $T(1, 4, 25)$ type torus bounding 10 families of Maslov index 2 holomorphic discs. The superpotential is given by $W_{T(1,4,25)} = u + 2\frac{e^{-\Lambda}}{u^2}(1 + w)^2 + \frac{e^{-2\Lambda}}{u^5 w}(1 + w)^5$.

Chapter 4

The exotic torus

This chapter is devoted to the actual construction of the exotic torus. Heuristically, we try to mimic the following procedure: first perform a nodal trade in a smooth corner of the moment polytope of $\mathbb{CP}(1, 1, 4)$ to get an "orbifold almost toric fibration"; then we smooth the orbifold singularity and trade it for an interior node, obtaining the almost toric fibration described by the middle diagram of Figure 3.1. This way the analogue of a Chekanov type torus in $\mathbb{CP}(1, 1, 4)$ deforms to a $T(1, 4, 25)$ type torus. For the first step, we consider a symplectic fibration on $\mathbb{CP}(1, 1, 4)$ given by $f_0(\tilde{x} : 1 : \tilde{z}) = \tilde{x}\tilde{z}$, with fibers preserved by a circle action $e^{i\theta} \cdot (\tilde{x} : 1 : \tilde{z}) = (e^{-i\theta}\tilde{x} : 1 : e^{i\theta}\tilde{z})$. The parallel transport of an orbit along a circle centered at $c \in \mathbb{R}_{>0}$ with radius $r < c$ is then a 'Chekanov type torus in $\mathbb{CP}(1, 1, 4)$'. The second part is carried out using a degeneration from $\mathbb{CP}^2$ to $\mathbb{CP}(1, 1, 4)$ parametrized by a real parameter t. We then consider a family of symplectic fibrations f_t on $\mathbb{CP}^2 \setminus \{y = 0\}$ converging to f_0, compatible with a circle action, so that, for each $t > 0$, the parallel transport of an orbit along the same circle at the base is a $T(1, 4, 25)$ type torus which converges to a 'Chekanov type torus in $\mathbb{CP}(1, 1, 4)$ as $t \to 0$. One technical issue that arrises is that we need to equip $\mathbb{CP}^2$ with a non-standard Kähler form (symplectomorphic to the standard one) in order to be able to give explicit descriptions of these tori.

As mentioned in the introduction, the projective plane degenerates to weighted projective spaces $\mathbb{CP}(a^2, b^2, c^2)$, where (a, b, c) is a Markov triple. For $c' = 3ab - c$, a deformation from $\mathbb{CP}(a^2, b^2, c^2)$ to $\mathbb{CP}(a^2, b^2, c'^2)$ can be seen explicitly inside $\mathbb{CP}(a^2, b^2, c, c')$ via the equation , $z_0 z_1 - (1 - t)z_2^{c'} - tz_3^c = 0$.

We are going to work only with $\mathbb{CP}^2 = \mathbb{CP}(1, 1, 1)$ and $\mathbb{CP}(1, 1, 4)$ inside $\mathbb{CP}(1, 1, 1, 2)$. For $t \in [0, 1]$, let X_t be the surface $z_0 z_1 - (1 - t)z_2^2 - tz_3 = 0$.

Explicit embeddings are

$$
\begin{aligned}
\mathbb{CP}(1, 1, 1) &\longrightarrow \mathbb{CP}(1, 1, 1, 2) \\
(x : y : z) &\mapsto (x : y : z : \frac{xy - (1 - t)z^2}{t}) \qquad \text{for} \quad t \neq 0, \qquad (4.1)
\end{aligned}
$$

$$\mathbb{CP}(1,1,4) \longrightarrow \mathbb{CP}(1,1,1,2)$$
$$(\tilde{x}:\tilde{y}:\tilde{z}) \mapsto (\tilde{x}^2:\tilde{y}^2:\tilde{x}\tilde{y}:\tilde{z}) \qquad \text{for } t = 0. \tag{4.2}$$

Set $\xi = \frac{xy - (1-t)z^2}{t}$. We now consider a fibration given by $F = \frac{z_2 z_3}{z_1^3}$ from $\mathbb{CP}(1,1,1,2)$ (minus two lines) to $\mathbb{CP}^1$, coinciding with f_0 on $X_0 \cong \mathbb{CP}(1:1:4)$. We restrict F to X_t, for $t > 0$, obtaining:

$$f_t : X_t \setminus \{(1:0:0:0)\} \simeq \mathbb{CP}^2 \setminus \{(1:0:0)\} \to \mathbb{CP}^1$$

$$f_t(x:y:z) = \frac{z\xi}{y^3} \tag{4.3}$$

Also consider the divisor $D = f_t^{-1}(c)$, where we take c to be a positive real number, thought of as a smoothing of $f_t^{-1}(0) = \{z\xi = 0\}$. We can define a circle action on $\mathbb{CP}^2 \setminus \{y = 0\}$, given, using coordinates $(z, \xi = \frac{x - (1-t)z^2}{t})$, by $e^{i\theta} \cdot (z, \xi) = (e^{-i\theta}z, e^{i\theta}\xi)$. This action does not extend to all of $\mathbb{CP}^2$, and it does not preserve the Fubini-Study Kähler form. However, we can modify the Kähler form to make it S^1-invariant in a open subset; see below. As in Example 2.1, we can consider Lagrangian $T(1,4,25)$ type tori, built up as the parallel transport of orbits along the circle centered at c with radius $r < c$. The other parameter of this fibration of Lagrangian tori is given by the moment map of the circle action (with respect to the modified Kähler form). In order to make everything explicit and be able to actually compute the Maslov index 2 holomorphic discs bounded by these tori, we will construct a Kähler form ω, for which the moment map is given by:

$$\mu_\omega(x:1:z) = 2\frac{|z|^2 - |\xi|^2}{1 + |z|^2 + |\xi|^2}, \tag{4.4}$$

on an open set contained in the inverse image with respect to f_t of an open disc of radius $R > 2c$ centered at 0.

For that, on the region described above, we take ω to be equal to $\frac{i}{4}\partial\bar{\partial}\log(1 + |z|^2 + |\xi|^2)$, in the coordinate chart $y = 1$. In homogeneous coordinates this form is given by

$$\tilde{\omega} = \frac{i}{4}\partial\bar{\partial}\log\left(1 + \left|\frac{z}{y}\right|^2 + \left|\frac{\xi}{y^2}\right|^2\right) = \frac{i}{4}\partial\bar{\partial}\log(|y|^4 + |z|^2|y|^2 + |\xi|^2) \tag{4.5}$$

The second expression is well defined on $\mathbb{CP}^2 \setminus (1:0:0)$, and equal to the first one since $\partial\bar{\partial}\log(|y|^4) = 0$. A calculation in the affine chart $x = 1$ shows that, along the complex line $y = 0$, it becomes $dy \wedge d\bar{y} / \left|\frac{(1-t)z}{t}\right|^2$. So we see that $\tilde{\omega}$ is well defined and nondegenerate away from $y = 0$, but it is degenerate along the line $y = 0$, and also is singular at $(1:0:0)$.

In order to define a nearby symplectic form, set $\rho = \left|\frac{z\xi}{y^3}\right|$ and $\ell = \frac{\left|\frac{z}{y}\right|^2 - \left|\frac{\xi}{y^2}\right|^2}{1 + \left|\frac{z}{y}\right|^2 + \left|\frac{\xi}{y^2}\right|^2}$ for $y \neq 0$,

and consider a cut off function η that is zero for $(x : y : z) \in \{\rho < R; |\ell| < \lambda_0\}$ and one for $(x : y : z) \in \mathbb{CP}^2 \setminus \{\rho \leq 2R; |\ell| \leq 2\lambda_0\}$. The parameters R and λ_0 are chosen so that $c + r < 2c < R$ and $0 < \lambda_0 < 1/2$, this way $\mathbb{CP}^2 \setminus \{\rho \leq 2R; |\ell| \leq 2\lambda_0\}$ is an open neighborhood of $\{y = 0\}$. Define

$$\omega = \frac{i}{4}\partial\bar{\partial}\log(|y|^4 + |z|^2|y|^2 + |\xi|^2 + s^2\eta(\rho, \ell)(|x|^2 + |y|^2 + |z|^2)^2) \tag{4.6}$$

where s is a very small constant. We see that ω is well defined in the whole $\mathbb{CP}^2$ since it is an interpolation between $\tilde{\omega}$ and the Kähler form $\omega_s = \frac{i}{4}\partial\bar{\partial}log(|y|^4 + |z|^2|y|^2 + |\xi|^2 + s^2(|x|^2 + |y|^2 + |z|^2)^2)$ which is $1/2$ of the pullback of the Fubini-Study form on $\mathbb{CP}^{11}$ via the embedding,

$$\iota : \mathbb{CP}^2 \longrightarrow \mathbb{CP}^{11}$$
$$(x : y : z) \mapsto (y^2 : zy : \xi : sx^2 : sy^2 : sz^2 : sxy : sxy : syz : syz : szx : szx)$$

Proposition 4.0.2. *For $s > 0$ sufficiently small, keeping fixed the other parameters c, r, t, $0 < \lambda_0 < 1/2$ and R, ω is a well defined nondegenerate Kähler form. Moreover, ω lies in the same cohomology class as the Fubini-Study form ω_{FS}.*

Proof. We note that for $y \neq 0$,

$$\omega = \frac{i}{4}\partial\bar{\partial}log((1 - \eta)\varphi_1 + \eta\varphi_2) = \frac{1}{2}dd^c log((1 - \eta)\varphi_1 + \eta\varphi_2),$$

where

$$\varphi_1 = \frac{|y|^4 + |z|^2|y|^2 + |\xi|^2}{|y|^4},$$

$$\varphi_2 = \frac{|y|^4 + |z|^2|y|^2 + |\xi|^2 + s^2(|x|^2 + |y|^2 + |z|^2)^2}{|y|^4},$$

and on a neighborhood of $y = 0$, ω is equal to ω_s, hence it is Kähler.

We already know ω is nondegenerate at $\{\rho < R; |\ell| < \lambda_0\}$ and $\mathbb{CP}^2 \setminus \{\rho \leq 2R; |\ell| \leq 2\lambda_0\}$. Since ω_s converges to $\tilde{\omega}$ uniformly on the compact set $\{\rho \leq 2R; |\ell| \leq 2\lambda_0\}$ (where $\tilde{\omega}$ is nondegenerate) as $s \to 0$, there is a small enough s making ω nondegenerate.

To determine the cohomology class of ω, it is enough to compute $\int_{[\mathbb{CP}^1]} \omega$. Considering $[\mathbb{CP}^1] = \{y = 0\}$ we see that $\int_{[\mathbb{CP}^1]} \omega = \int_{[\mathbb{CP}^1]} \omega_s$ and so $[\omega] = [\omega_s] = \frac{1}{2}\iota^*[\omega_{\mathbb{CP}^{11}}] = [\omega_{FS}]$. $\qquad\square$

The space of Kähler forms in the same cohomology class is connected. Hence, by Moser's theorem, $(\mathbb{CP}^2, \omega)$ and $(\mathbb{CP}^2, \omega_{FS})$ are symplectomorphic. After applying such a symplecto-morphism, we get Lagrangian tori in $(\mathbb{CP}^2, \omega_{FS})$ with the same properties as the ones we consider in $(\mathbb{CP}^2, \omega)$.

The constants c, r, t, λ_0, R and s are chosen in this order. For what follows c, $0 < \lambda_0 < 1/2$ and $R > 2c$ are fixed, $r < c$ and t is thought to be very small with respect to c and r. Considering the symplectic form ω from now on, we define the following Lagrangian tori:

Definition 4.0.3. *For $\lambda \in \mathbb{R}$, $|\lambda| < \lambda_0$:*

$$T_{r,\lambda}^c = \left\{ (x : y : z) \in \mathbb{CP}^2; \left| \frac{z\xi}{y^3} - c \right| = r, \ \frac{\mu_\omega}{2} = \frac{\left| \frac{z}{y} \right|^2 - \left| \frac{\xi}{y^2} \right|^2}{1 + \left| \frac{z}{y} \right|^2 + \left| \frac{\xi}{y^2} \right|^2} = \lambda \right\}. \tag{4.7}$$

For the sake of using Lemma 2.1.4, which gives a convenient formula for computing Maslov index for *special* Lagrangian submanifolds, we now consider the meromorphic 2-form on $\mathbb{CP}^2$ which is the quotient of $\Omega_{\mathbb{C}^3} = \frac{dx \wedge dy \wedge dz}{t(\xi z - cy^3)}$ defined on $\mathbb{C}^3$ and has poles on the divisor D. On the complement of $\{y = 0\}$, taking $y = 1$, it is given by

$$\Omega = \frac{dx \wedge dz}{t(\xi z - c)} = \frac{d\xi \wedge dz}{\xi z - c}. \tag{4.8}$$

Here $\xi = \frac{x - (1-t)z^2}{t}$.

Proposition 4.0.4. *For c, r and λ as above, the tori described in the (ξ, z) coordinate chart by $T_{r,\lambda}^c = \{(\xi, z); |\xi z - c| = r; |z|^2 - |\xi|^2 = \lambda(1 + |z|^2 + |\xi|^2)\}$ are special Lagrangian with respect to Ω.*

Proof. Take V_H the Hamiltonian vector field of the Hamiltonian $H(\xi, z) = |\xi z - c|^2$, i.e., defined via $\omega(V_H, \cdot) = dH$. Since H is constant on the Lagrangian $T_{r,\lambda}^c$ and on each symplectic fiber of $f(\xi, z) = \xi z$, V_H is symplectically orthogonal to both, hence tangent to the Lagrangian $T_{r,\lambda}^c$ and not tangent to the symplectic fibers of f. Consider the vector field $\vartheta = (i\xi, -iz)$, tangent to the fibers and the Lagrangian torus, as they intersect along circles of the form $(e^{i\theta}\xi_0, e^{-i\theta}z_0)$. So, $\{\vartheta, V_H\}$ form a basis for the tangent space of $T_{r,\lambda}^c$. Now note that

$$\iota_\vartheta \Omega = \frac{i\xi dz + iz d\xi}{\xi z - c} = id\log(\xi z - c).$$

Therefore,

$$Im(\Omega)(\vartheta, V_H) = d\log|\xi z - c|(V_H) = 0.$$

$\square$

Chapter 5

Computing holomorphic discs in $\mathbb{CP}^2$ bounded by $T^c_{r,0}$

In this chapter we focus on the case $\lambda = 0$ and show that, at least for small enough t with respect to r and c, it bounds the expected 10 different families of Maslov index 2 holomorphic discs (with the expected multiplicity modulo signs). We often use the coordinates $(z_0 : z_1 : z_2 : z_3)$, but restricted to $\mathbb{CP}^2 \simeq X_t$ via the embedding (4.1).

5.1 The homology classes

We omit the subindex t and consider $f(x : y : z) = \frac{z\xi}{y^3}$ mapping $\mathbb{CP}^2$ minus $(1 : 0 : 0)$ to $\mathbb{CP}^1$.

Proposition 5.1.1. *There is only one family of holomorphic discs, up to reparametrization, in $\mathbb{CP}^2$ with boundary on $T^c_{r,0}$ ($r < c$) that is mapped injectively to the disc $|w - c| \leq r$ by f, where w is the coordinate in $\mathbb{C}$.*

Proof. Let $u : \mathbb{D} \to \mathbb{CP}^2$ be such a disc so, up to reparametrization, $f \circ u(w) = \Psi(w) = rw + c$. The map u can be described using coordinates $y = z_1(w) = 1$, $z = z_2(w)$ and $\xi = z_3(w)$, so $z_2(w)z_3(w) = \Psi(w)$. Since zero (and infinity) does not belong to the image of Ψ as $r < c$, z_2 and z_3 have no zeros or poles on the disc (note that if $z(w) = 0$ and $\xi(w) = \infty$ then $x(w) = \infty$, contradicting $y(w) \neq 0$, for the same reason $z(w) \neq \infty$). At the boundary of the disc, mapped by u to $T^c_{r,0}$, $|z_2| = |z_3|$. So, by holomorphicity, $z_2(w) = e^{i\theta}z_3(w) = e^{i\frac{\theta}{2}}\sqrt{\Psi(w)}$, for some choice of square root and some constant θ. $\qquad\square$

Call β the relative homotopy class of the above family of discs, α the class of the Lefschetz thimble associated to the critical point of f at the origin lying above the segment $[0, c - r]$ (oriented to intersect positively $\{z = 0\}$) and $H = [\mathbb{CP}^1]$ the image of the generator of $\pi_2(\mathbb{CP}^2)$ in $\pi_2(\mathbb{CP}^2, T^c_{r,0})$. One checks that α, β, H form a basis of $\pi_2(\mathbb{CP}^2, T^c_{r,0})$. On Figure 3.4, holomorphic discs in the class β are represented by the tropical disc arriving at the torus

in the direction $(1,0)$ and associated to the term u of the superpotential $W_{T(1,4,25)}$. If we consider $\lambda > 0$, and increase $r \to c$, we see that the torus depicted on Figure 3.4 approaches the wall, and the class α corresponds to a tropical Maslov index 0 disc that runs along the wall and ends at the node.

In order to understand what relative homotopy classes are allowed to have Maslov index 2 holomorphic discs, we analyze their intersection with some other complex curves, for instance the line over ∞, $y = 0$, the line and conic over 0, $z = 0$ and $D_2 : xy - (1-t)z^2 = 0$. Another curve we use is a quintic, D_5 that converges to $(\tilde{x}\tilde{z} - c\tilde{y}^5)^2 = 0$ on $\mathbb{CP}(1,1,4)$. It is given by

$$D_5 : z_0 z_3^2 - 2c z_1^2 z_2 z_3 + c^2 z_1^5 = x\xi^2 - 2cy^2 z\xi + c^2 y^5 = 0$$

For $z \neq 0$ and setting $f = \frac{z\xi}{y^3}$, we can write this equation as

$$y^5 \left(c^2 - 2cf + \frac{xy}{z^2} f^2 \right) = 0 \tag{5.1}$$

Remark 5.1.2. *Again relating to Figure 3.4, the leftmost node is thought to be the torus* $T^c_{c,0}$ *and the wall in the direction* $(1,-1)$ *to be formed by the tori* $T^c_{c,\lambda}$. $D_2 = \{\xi = 0\}$ *projects to the upper part of the wall, while* $\{z = 0\}$ *projects to the lower part of the same wall, as the Maslov index 0 discs bounded by* $T^c_{c,\lambda}$ *are contained in these two divisors. Using similar reasoning, one expects that over the rightmost wall lie complex curves converging to* $\{\tilde{y}(\tilde{x}\tilde{z} - c\tilde{y}^5) = 0\}$, *the boundary divisor of the "orbifold almost toric fibration" on* $\mathbb{CP}(1,1,4)$. D_5 *converges to* $\{(\tilde{x}\tilde{z} - c\tilde{y}^5)^2 = 0\}$, *hence it is thought to lie over the lower part of the rightmost wall, while* $\{y = 0\}$, *which converges to* $\{\tilde{y}^2 = 0\}$, *is thought to lie over the upper part of the same wall.*

Remark 5.1.3. *To compute intersection number with* H *in Figure 3.4, one can use the tropical rational curve formed by the union of all the tropical discs depicted on Figure 3.2. Also, note that each wall hits the cut of the other, leaving them with slopes* $(-5,2)$ *on the top left and* $(7,2)$ *on the top right; the additional dotted lines are omitted on all pictures for simplicity.*

Lemma 5.1.4. *For fixed c and* $r < c$, *and for t sufficiently small, the classes* α, β *and* H *intersect the varieties* $\{z = 0\}$, $\{y = 0\}$, $D_3 = f^{-1}(c) \cup \{(1 : 0 : 0)\}$, $D_2 : xy - (1-t)z^2 = 0$, D_5 *and have Maslov index, according to the table below.*

Class	$z = 0$	$y = 0$	D_3	D_2	D_5	*Maslov index* μ
α	*1*	*0*	*0*	*-1*	*0*	*0*
β	*0*	*0*	*1*	*0*	*2*	*2*
H	*1*	*1*	*3*	*2*	*5*	*6*

Proof. In order to use these curves to compute intersection numbers, we first need to ensure they don't intersect $T^c_{r,0}$. This is clear for $z = 0$, $y = 0$, D_3, and D_2. Later we will see that $T^c_{r,0} \cap D_5 = \emptyset$.

The intersections with H follow from Bezout's Theorem. By construction, α (represented by the Lefschetz thimble over the segment $[0, c - r]$ which can be parametrized by $y = 1$,

$z = \rho e^{i\theta}$, $\xi = \rho e^{-i\theta}$, $\rho \in [0, c - r]$) does not intersect $y = 0$ and D_3, also, it intersects both $z = 0$ and D_2 at one point with multiplicity 1 and -1, respectively. Each disc computed in Proposition 5.1.1 representing the class β does not intersect $z = 0$, $y = 0$, and D_2, and intersect D_3 positively at one point.

It remains for us to understand the intersection of D_5 with the torus $T_{r,0}^c$, α and β. For that, we look at the family of conics $\mathcal{C} = \{z = e^{i\theta}\xi;\ \theta \in [0, 2\pi]\}$ containing $T_{r,0}^c$, the thimble representing the class α and the discs representing the class β computed in Proposition 5.1.1.

On $\mathcal{C}$, using the coordinate chart $y = 1$, we have:

$$z = e^{i\theta}\xi = e^{i\theta}\frac{x - (1 - t)z^2}{t}. \tag{5.2}$$

So, solving for x in (5.2), and using $f = z\xi = e^{-i\theta}z^2$, we get:

$$x = te^{-i\frac{\theta}{2}}f^{1/2} + (1 - t)e^{i\theta}f, \tag{5.3}$$

for some square root of f. Then, by (5.1) and (5.3), the points of $D_5 \cap \mathcal{C}$ are those where

$$c^2 - 2cf + e^{-i\theta}f(te^{i\frac{-\theta}{2}}f^{1/2} + (1 - t)e^{i\theta}f) = (f - c)^2 + tf^{3/2}(e^{-i\frac{3\theta}{2}} - f^{1/2}) = 0$$

For t small enough, for each value of θ, all the solutions of this equation lies in the region $|f - c| < r$. From this we can conclude that $D_5 \cap T_{r,0}^c = \emptyset$, $D_5 \cap \alpha = \emptyset$, since, in $T_{r,0}^c$, $|f - c| = r$ and the thimble representing α lies over $[0, c - r]$.

Now, a holomorphic disc representing the class β is given by $z = \xi = f^{1/2}$ and $Re(z) > 0$; see Proposition 5.1.1. This means that this disc intersects D_5 in exactly two points, namely the two solutions of $(z^2 - c)^2 + tz^3(e^{-i\frac{3\theta}{2}} - z) = 0$, where z is close to $\sqrt{c}$. As both are complex curves, the intersections count positively, so the intersection number between D_5 and β is equal to 2.

Finally, from lemma 2.1.4, we see that the Maslov index is twice the intersection with the divisor D_3.

□

Lemma 5.1.5. *The only classes in $\pi_2(\mathbb{CP}^2, T_{r,0})$ which may contain holomorphic discs of Maslov index 2 are β, $H - 2\beta + m\alpha$, $-1 \le m \le 2$ and $2H - 5\beta + k\alpha$, $-2 \le k \le 4$.*

Proof. To have Maslov index 2 the class must have the form $\beta + l(H - 3\beta) + k\alpha$. Considering positivity of intersections with $y = 0$ we get $l \ge 0$, with $z = 0$ and D_2 we get $-l \le k \le 2l$, and finally with D_5, $l \le 2$. □

5.2 Discs in classes $H - 2\beta + m\alpha$

Theorem 5.2.1. *There are no Maslov index 2 holomorphic discs in the class $H - 2\beta - \alpha$; there are one-parameter families of holomorphic discs in the classes $H - 2\beta$ and $H - 2\beta + 2\alpha$,*

with algebraic counts equal to 2 up to sign in both cases, and a one-parameter family of holomorphic discs in the class $H - 2\beta + \alpha$, with algebraic count equal to 4 up to sign.

This is precisely what we expect from the term $2\frac{e^{-\Lambda}}{u^2}(1+w)^2$ in $W_{T(1,4,25)}$; see equation (3.3).

Proof. We will try to find holomorphic discs $u : (\mathbb{D}, S^1) \to (\mathbb{CP}^2, T^c_{0,r})$ in the class $H - 2\beta + m\alpha$, $-1 \leq m \leq 2$. Recall $f : \mathbb{CP}^2 \setminus (0 : 0 : 1) \to \mathbb{CP}^1$, $f(x : y : z) = \frac{z\xi}{y^3}$, and set $\Psi = f \circ u : \mathbb{D} \to \mathbb{CP}^1$. Since u has Maslov index 2 it doesn't go through $(1 : 0 : 0)$, where D_3 has a self intersection, so Ψ is well-defined.

We look at $\frac{\Psi(w)-c}{r}$, which maps the unit circle to the unit circle. Looking at the intersection numbers given in Lemma 5.1.4, we see that our disc must intersect $y = 0$ and the divisor D_3 at 1 point. Therefore, as $\Psi = f \circ u$, $f^{-1}(\infty) = \{y^3 = 0\}$ and $D_3 = f^{-1}(c) \cup (1 : 0 : 0)$, the map $\frac{\Psi(w)-c}{r}$ has a pole of order 3 and a simple zero, so

$$\frac{\Psi(w) - c}{r} = \frac{\tau_{w_0}(w)}{\tau^3_{w_1}(w)}e^{i\phi}, \quad \text{where} \quad \tau_v(w) = \frac{w - v}{1 - \bar{v}w}, \tag{5.4}$$

for some w_0, w_1 in $\mathbb{D}$ and $e^{i\phi} \in S^1$. We can use automorphisms of the disc to assume $w_1 = 0$, $\phi = 0$ and write $w_0 = a$. Note that the disc automorphism $w \mapsto e^{i\phi'}w$ amounts to $w_0 \mapsto e^{-i\phi'}w_0$ and $\phi \mapsto \phi - 2\phi'$ in (5.4). So, $\phi' = \pi$ keeps $e^{i\phi}$ invariant, therefore we need to keep in mind that $\pm a$ gives the same holomorphic disc modulo reparametrization.
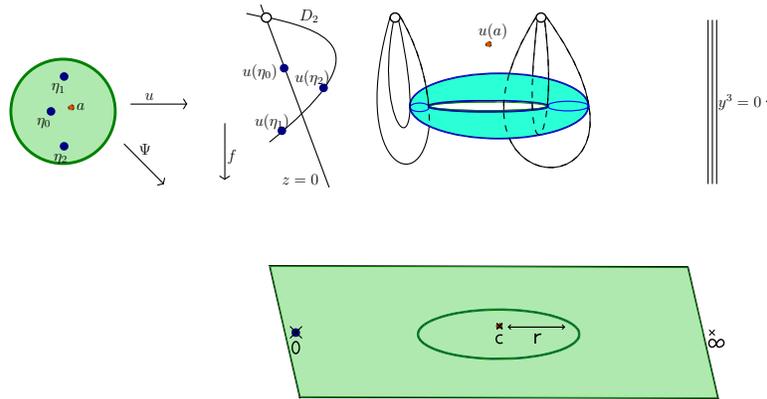
Figure 5.1: Picture of $\Psi(w) = f \circ u(w) = \frac{z(w)\xi(w)}{y^3(w)} = \frac{z_2(w)z_3(w)}{z^3_1(w)}$ (for the case $m = 0$; $|I| = 2$, i.e., u intersects the conic D_2 twice). $\{\eta_0, \eta_1, \eta_2\} = \Psi^{-1}(0)$ and $\{a\} = \Psi^{-1}(c)$ behave as in Lemma 5.2.3 for small t. Recall that the divisor D_3 is the closure of $f^{-1}(c) \ni u(a)$.

Since $r < c$, the image of u intersects $f^{-1}(0) \subset D_2 \cup \{z = 0\}$ in three points $u(\eta_j)$'s, j = 0, 1, 2, i.e., $\eta_j \in \mathbb{D}$ are so that $\Psi(\eta_j) = 0$. The integer m in $H - 2\beta + m\alpha$ determines how many times the disc u intersects D_2, and we consider a set $I \subset \{0, 1, 2\}$ with that number

of elements. Writing $z_1 = y$, $z_2 = z$ and $z_3 = \xi$, and $\tau_j = \tau_{\eta_j}$ we see that the map u can be expressed in the form

$$z_1(w) = w \ , \ z_2(w) = e^{-i\theta} h(w) \prod_{j \notin I} \tau_j(w) \ , \ z_3(w) = e^{i\theta} h(w) \prod_{j \in I} \tau_j(w), \tag{5.5}$$

where $h(w)$ is a nonvanishing holomorphic functions and $e^{i\theta} \in S^1$.

Remark 5.2.2. *A suitable scaling of the homogeneous coordinates eliminates the need for a multiplicative factor in the expression for $z_1(w)$. In principle we know that $z_2(w) = e^{-i\theta} h_2(w) \prod_{j \notin I} \tau_j(w)$, $z_3(w) = e^{i\theta} h_3(w) \prod_{j \in I} \tau_j(w)$. But we see that on $\partial \mathbb{D}$, $\left| \frac{z_2}{z_1} \right| = \left| \frac{z_3}{z_1^2} \right|$ and $|z_1| = 1$, so $|h_2| = |h_3|$ on the unit circle, therefore $h_3 = e^{i\theta'} h_2$ for some constant θ'. Note that we can absorb $-\theta'/2$ in θ and assume that $h_3 = h_2 = h$.*

Since $\Psi(w) = \frac{z_2(w) z_3(w)}{z_1^3(w)} = \frac{h^2(w) \prod \tau_j(w)}{w^3}$, we get $h(w) = \left(\frac{\Psi(w) w^3}{\prod \tau_j(w)} \right)^{1/2}$, for some choice of square root. The other choice is equivalent to a translation by π of the parameter θ. Rewriting this last equation and using $\frac{\Psi(w) - c}{r} = \frac{\tau_a(w)}{w^3}$, we get:

$$w^3 \Psi(w) = r\tau_a(w) + cw^3 = h^2(w) \tau_0(w) \tau_1(w) \tau_2(w). \tag{5.6}$$

We expect one parameter family(ies) of solutions and we see that u is determined by the parameters a and θ. Therefore we want to understand how many possible choices for a there are, for any given θ. Moreover, understanding how these solutions vary with θ, we can describe the moduli space of holomorphic discs in the class $H - 2\beta + m\alpha$ bounded by $T_{r,0}^c$, denoted by $\mathcal{M}(T_{r,0}^c, H - 2\beta + m\alpha)$, for each m.

The possible values of a are constrained by the following equation coming from the fact that $\xi = -\frac{(1-t)}{t} z^2$ when $y = 0$:

$$\frac{z_3(0)}{z_2^2(0)} = -\frac{1-t}{t} = \frac{e^{3i\theta} \prod_{j \in I} \tau_j(0)}{h(0) \prod_{j \notin I} \tau_j^2(0)} = \frac{e^{3i\theta} (-1)^{|I|} \prod_{j \in I} \eta_j}{h(0) \prod_{j \notin I} \eta_j^2}. \tag{5.7}$$

Since (5.6) implies that $-ar = -h^2(0) \eta_0 \eta_1 \eta_2$, (5.7) can be rewritten as

$$ar \left(\frac{1-t}{t} \right)^2 \prod_{j \notin I} \eta_j^3 = e^{6i\theta} \prod_{j \in I} \eta_j^3. \tag{5.8}$$

Note that solving (5.8) for a amounts to a solution of (5.7) for some choice of square root for $h(w) = \left(\frac{\Psi(w) w^3}{\prod \tau_j(w)} \right)^{1/2}$.

Understanding the behavior of the parameters η_j and a as $t \to 0$ will allow us to analyze the existence of a solving this equation for small values of t. Note that the right side of (5.8) is uniformly bounded for all t. So we conclude that $a \prod_{j \notin I} \eta_j \to 0$, as $t \to 0$. Moreover, if we can show that $h(0)$ is bounded away from zero, then we can conclude that $\eta_j \to 0$ for some $j \notin I$; see (5.7).

Lemma 5.2.3. $h(0)$ *is bounded away from 0 and, after possibly relabeling the η_j's, the following asymptotic hold as $t \to 0$:*

$$a = O(t^{1/2}), \ \eta_0 = O(t^{1/2}), \ \eta_1 \to \sqrt{\frac{r}{c}}i, \ \eta_2 \to -\sqrt{\frac{r}{c}}i.$$

Moreover, $0 \notin I$. Therefore, as $|I| < 3$ represents the number of intersection with D_2, there is no holomorphic disc in the class $H - 2\beta - \alpha$ (i.e. for $m = -1$).

Proof. Consider the polynomial:

$$\Xi(w) = w^3(1 - \bar{a}w)\Psi(w) = r(w - a) + cw^3(1 - \bar{a}w) = -c\bar{a}(w - \zeta)(w - \eta_0)(w - \eta_1)(w - \eta_2),$$

for some ζ, with $|\zeta| > 1$. Assume $|\eta_0| \le |\eta_1|$, $|\eta_0| \le |\eta_2|$, and write

$$(w - \eta_0)(w - \eta_1)(w - \eta_2) = w^3 - \sigma w^2 + qw - p$$

By comparing coefficients, we get

$$p\zeta = \frac{ra}{c\bar{a}} \tag{5.9}$$

$$1 = \bar{a}(\zeta + \sigma) \tag{5.10}$$

By (5.6),

$$h^2(0) = \frac{ar}{\eta_0\eta_1\eta_2} = \frac{ar}{p}.$$

By equations (5.9), (5.10) and noting that $|\sigma| \le 3 \le 3|\zeta|$,

$$1 = |a||\zeta + \sigma| \le 4|a\zeta| = \frac{4|a|r}{c|p|} = \frac{4|h^2(0)|}{c}.$$

So, we get $|h(0)| \ge \frac{\sqrt{c}}{2}$. Looking at equation (5.7), we get that at least one η_j must be in the denominator. More precisely $\prod_{j \notin I} \eta_j = O(t^{1/2})$. As the other η_j's lie in the unit disc, $p = O(t^{1/2}) \to 0$ and by (5.9), $\zeta \mapsto \infty$. Also by (5.10) , as σ is bounded, we get that $a \mapsto 0$, in fact $a = O(t^{1/2})$.

Therefore,

$$\Xi(w) = w(cw^2 + r) + w^4 O(t^{1/2}) + O(t^{1/2}),$$

and we see that $\eta_0 = O(t^{1/2})$ and $\eta_1\eta_2 \mapsto \frac{r}{c}$, say $\eta_1 \mapsto +\sqrt{\frac{r}{c}}i$, $\eta_2 \mapsto -\sqrt{\frac{r}{c}}i$. In particular, we conclude that $0 \notin I$. Also, $p\zeta = \zeta\eta_0\eta_1\eta_2 = \zeta\eta_0(\frac{r}{c} + O(t^{1/2})) = \frac{ra}{c\bar{a}}$, hence $\zeta\eta_0 = \frac{a}{\bar{a}} + O(t^{1/2})$. Note that since $|I| < 3$, there are no holomorphic discs for $m = -1$, and this finishes the proof of Lemma 5.2.3.

$\square$

Now we need to analyze the cases $I = \emptyset, \{1\}, \{2\}, \{1, 2\}$.

Case $I = \emptyset$, $m = 2$:

By (5.8), (5.9):

$$(\bar{a}\zeta)^3 = a^4 \left(\frac{1-t}{t}\right)^2 \frac{e^{-6\theta i} r^4}{c^3} = a^4 K \tag{5.11}$$

where $K = \left(\frac{1-t}{t}\right)^2 \frac{e^{-6\theta i} r^4}{c^3}$.

Proposition 5.2.4. *For small enough $t > 0$, equation (5.11) has four solutions for each given parameter θ. Moreover, naming these solutions $a_1(\theta)$, $a_2(\theta)$, $a_3(\theta)$, $a_4(\theta)$, as we vary continuously with θ, in counter-clockwise order, we have that $a_j(\theta + \pi/3) = a_{j+1}(\theta)$.*

Proof. By (5.10)

$$(\bar{a}\zeta)^3 = 1 + O(t^{1/2}) \tag{5.12}$$

Combining (5.11) with (5.12) we see that for $g(a) = 1 - (\bar{a}\zeta)^3$

$$a^4 K - 1 + g(a) = 0 \tag{5.13}$$

One sees that, for sufficiently small t, there are 4 solutions of such equation since $g(a)$ and $g'(a)$ are $O(t^{1/2})$. (To see that $g'(a) = O(t^{1/2})$, we use that $g(a) = \tilde{g}(a, \bar{a})$, where $\tilde{g}(a, b)$ is a holomorphic function, and using Cauchy's differentiation formula, we get that each partial derivative is $O(t^{1/2})$.)

So for each θ there are four solutions for a, each of them close to a fourth root of K^{-1}. Recall we named these solutions, as varying continuously with θ, in counter-clockwise order, $a_1(\theta)$, $a_2(\theta)$, $a_3(\theta)$, $a_4(\theta)$. We see from (5.11) that $a_j(\theta + \pi/3) = a_{j+1}(\theta)$. $\qquad\square$

Let $u^\theta_{a_1(\theta)}$ be the holomorphic disc given by (5.5), for a given value of θ and the other parameters determined by $a_1(\theta)$.

Lemma 5.2.5. *The moduli space of holomorphic discs in the class $H - 2\beta + 2\alpha$, $\mathcal{M}(T^c_{r,0}, H - 2\beta + 2\alpha)$, can be parametrized using only holomorphic discs $u^\theta_{a_1(\theta)}$ for $\theta \in [0, 2\pi]$. Also, the algebraic count of holomorphic discs in $\mathcal{M}(T^c_{r,0}, H - 2\beta + 2\alpha)$, $n_{H-2\beta+2\alpha}(T^c_{r,0})$, is equal to 2 up to sign.*

Proof. Since $a_j(\theta + \pi/3) = a_{j+1}(\theta)$, we can parametrize the moduli space of holomorphic discs in the class $H - 2\beta + 2\alpha$ using only holomorphic discs $u^\theta_{a_1(\theta)}$ for $\theta \in [0, 4\pi]$. But recall that solutions are counted twice as the disc automorphism $w \mapsto -w$ amounts to $a \mapsto -a$ and $0 = \phi \mapsto \phi - 2\pi = -2\pi$ in (5.4). Hence we see that $u^{\theta+2\pi}_{a_1(\theta+2\pi)} = u^\theta_{a_3(\theta)} = u^\theta_{-a_1(\theta)}$ is the same up to reparametrization. Therefore the map $\theta \mapsto u^\theta_{a_1(\theta)}$, from $S^1 = [0, 2\pi]/0 \sim 2\pi$ to the moduli space $\mathcal{M}(T^c_{r,0}, H - 2\beta + 2\alpha)$ gives a diffeomorphism.

In order to compute $n_{H-2\beta+2\alpha}(T^c_{r,0})$ we need to look at $ev_*[\mathcal{M}(T^c_{r,0}, H - 2\beta + 2\alpha)] = n_{H-2\beta+2\alpha}(T^c_{r,0})[T^c_{r,0}]$. The boundary of each holomorphic disc lies in the class $2(\partial\alpha - \partial\beta)$, and the parameter θ comes from the action $e^{i\theta}\cdot(\xi, z) = (e^{i\theta}\xi, e^{-i\theta}z)$, described in coordinates (ξ, z) for $y = 1$, whose orbits are in the class of the thimble, i.e., $\partial\alpha$. Therefore, $n_{H-2\beta+2\alpha}(T^c_{r,0}) = \pm 2$.

$\square$

Case $I = \{2\}$ (similarly $I = \{1\}$) , $m = 1$:

By (5.8), (5.9), setting now $K = \left(\frac{1-t}{t}\right)^2 re^{-6\theta i}$:

$$K\eta_0^3 = \frac{1}{a}\frac{\eta_2^3}{\eta_1^3} = \frac{1}{a}(-1 + O(t^{1/2})). \tag{5.14}$$

Similarly to the previous case we have

Proposition 5.2.6. *For small enough $t > 0$, equation (5.14) has four solutions for each given parameter θ. Moreover, naming these solutions $a_1(\theta)$, $a_2(\theta)$, $a_3(\theta)$, $a_4(\theta)$, as we vary continuously with θ, in counter-clockwise order, we have that $a_j(\theta + \pi/3) = a_{j+1}(\theta)$.*

Lemma 5.2.7. *The moduli space of holomorphic discs in the class $H - 2\beta + \alpha$, $\mathcal{M}(T^c_{r,0}, H - 2\beta + \alpha)$, can be parametrized using only holomorphic discs $u^\theta_{a_1(\theta)}$ for $\theta \in [0, 4\pi]$. Moreover, the algebraic count of holomorphic discs in $\mathcal{M}(T^c_{r,0}, H - 2\beta + \alpha)$, $n_{H-2\beta+\alpha}(T^c_{r,0})$, is equal to 4 up to sign.*

Proof. (*of Proposition 5.2.6 and of Lemma 5.2.7*)
Since $\zeta\eta_0 = \frac{a}{\bar{a}} + O(t^{1/2})$, and $a = O(t^{1/2})$:

$$(\bar{a}\zeta)^3\frac{1}{a}(-1 + O(t^{1/2})) = K(\bar{a}\zeta\eta_0)^3 = K[a(1 + O(t^{1/2}))]^3 = Ka^3(1 + O(t^{1/2})).$$

Using $(\bar{a}\zeta)^3 = 1 + O(t^{1/2})$, we get

$$Ka^4 + O(t^{1/2}) = -1. \tag{5.15}$$

Using the same argument as before we get four solutions for a, $a_1(\theta)$, $a_2(\theta)$, $a_3(\theta)$, $a_4(\theta)$, varying continuously with θ, ordered in the counter-clockwise direction. Again $a_j(\theta+\pi/3) = a_{j+1}(\theta)$, but now the disc automorphism $w \mapsto -w$, not only switches $a \mapsto -a$ but also $\eta_1 \leftrightarrow \eta_2$, which accounts for the case $I = \{1\}$. Therefore the moduli space $\mathcal{M}(T^c_{r,0}, H-2\beta+\alpha)$ is given by $\{u^\theta_{a_1(\theta)}; \theta \in [0, 4\pi]\}$, and hence $n_{H-2\beta+\alpha}(T^c_{r,0}) = \pm 4$. $\square$

The case $I = \{1, 2\}$, $m = 0$, works in a totally analogous way, with $n_{H-2\beta}(T^c_{r,0}) = \pm 2$. This concludes the proof of Theorem 5.2.1. $\square$

5.3   Discs in classes $2H - 5\beta + k\alpha$

Theorem 5.3.1. *There are no Maslov index 2 holomorphic discs in the class $2H - 5\beta - 2\alpha$, and one-parameter families of holomorphic discs in the classes $2H - 5\beta + k\alpha$, $k = -1, 0, 1, 2, 3, 4$, with algebraic counts equal to $1, 5, 10, 10, 5, 1$, up to sign, respectively.*

This is precisely what we expect from the term $\frac{e^{-2\Lambda}}{u^5 w}(1+w)^5$ in $W_{T(1,4,25)}$; see equation (3.3).

Proof. We start approaching the problem following the same reasoning as in the previous subsection. But we will get an extra parameter, since the intersection with $\{y = 0\}$ is 2 for discs in the classes $2H - 5\beta + k\alpha$, $-2 \leq k \leq 4$. This will make our computation harder. Nonetheless, looking at Figure 3.4, for $t \to 0$ we expect the discs in these classes (for $k \geq -1$) to converge to holomorphic discs in $\mathbb{CP}(1,1,4)$ that remain away from the orbifold point, since they don't touch the singular fiber that collapses into the singular orbifold point when $t = 0$. The idea is then to understand the limits of such discs when $t \to 0$, 'count' them for $t = 0$ and use Lemma 5.3.6 to show that the count remains the same for small $t > 0$.

Consider a holomorphic map $u : (\mathbb{D}, S^1) \to (\mathbb{CP}^2, T_{0,r}^c)$ in the class $2H - 5\beta + k\alpha$, $-2 \leq k \leq 4$, and $\Psi(w) = f \circ u(w)$. Analyzing intersection numbers with divisors we get

$$\frac{\Psi(w) - c}{r} = \frac{\tau_{w_0}(w)}{\tau_{w_1}^3(w)\tau_{w_2}^3(w)}e^{i\phi} \tag{5.16}$$

and denote by $\eta_0, \ldots, \eta_5$ the zeros of $\Psi(w)$. Again using automorphisms of the disc we can choose $w_1 = 0$ and $\phi = 0$ and also rename $w_2 = \nu$ and $w_0 = b$. Then, the holomorphic disc can be described by

$$z_1(w) = w\tau_\nu(w) \ , \ \ z_2(w) = e^{-i\theta}h(w)\prod_{j \notin I}\tau_j(w) \ , \ \ z_3(w) = e^{i\theta}h(w)\prod_{j \in I}\tau_j(w) \tag{5.17}$$

where $h(w) = \left(\frac{\Psi(w)w^3\tau_\nu^3(w)}{\prod \tau_j(w)}\right)^{1/2}$, and $I \subset \{0, 1, 2, 3, 4, 5\}$. Recall that $y = z_1$, $z = z_2$, $\xi = z_3$ and $\tau_j = \tau_{\eta_j}$.

In the same way as in the previous section, we get a pair of equations

$$\frac{z_3(0)}{z_2^2(0)} = -\frac{1-t}{t} = \frac{e^{3i\theta}\prod_{j \in I}\tau_j(0)}{h(0)\prod_{j \notin I}\tau_j^2(0)} = \frac{e^{3i\theta}(-1)^{|I|}\prod_{j \in I}\eta_j}{h(0)\prod_{j \notin I}\eta_j^2} \tag{5.18}$$

$$\frac{z_3(\nu)}{z_2^2(\nu)} = -\frac{1-t}{t} = \frac{e^{3i\theta}\prod_{j \in I}\tau_j(\nu)}{h(\nu)\prod_{j \notin I}\tau_j^2(\nu)} = \frac{e^{3i\theta}\prod_{j \in I}q_j}{h(\nu)\prod_{j \notin I}q_j^2} \tag{5.19}$$

where we write $q_j = \tau_j(\nu)$. Again we want to understand the asymptotic of the parameters b, ν and η_j as $t \to 0$.
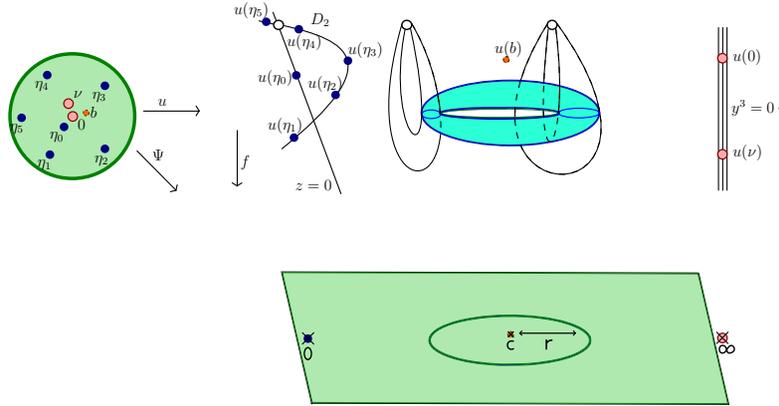
Figure 5.2: Picture of $\Psi(w) = f \circ u(w) = \frac{z(w)\xi(w)}{y^3(w)} = \frac{z_2(w)z_3(w)}{z_1^3(w)}$ (for the case $k = -1$; $|I| = 4$, i.e., u intersects the conic D_2 in five points). $\{\eta_0, \cdots, \eta_5\} = \Psi^{-1}(0)$, $\{0, \nu\} = \Psi^{-1}(\infty)$ and $\{b\} = \Psi^{-1}(c)$ behave as in Lemma 5.3.2 for small t. Recall that the divisor D_3 is the closure of $f^{-1}(c) \ni u(b)$.

Lemma 5.3.2. *$h(0)$ is bounded away from 0 and, after possibly relabeling the η_j's, the following asymptotics hold as $t \to 0$:*

$$b = O(t^{1/2}), \ \nu = O(t^{1/2}), \ \eta_0 = O(t^{1/2}) \ \text{and for } j \neq 0, \ \eta_j \to -\frac{r^{\frac{1}{5}}}{c}e^{\frac{2\pi i}{5}j}.$$

Using (5.18) and the above Lemma 5.3.2 we see that $0 \notin I$. Therefore there is no holomorphic disc representing the class $2H - 5\beta + k\alpha$, for $k = -2$. To prove the existence of such discs for $-1 \leq k \leq 4$ with the right count, we look at the limit $t = 0$, i.e., in $\mathbb{CP}(1:1:4)$. These six families of discs are expected to 'survive' in the limit and not pass through the orbifold point of $\mathbb{CP}(1,1,4)$; see Figure 3.4. We show that this is the case for the limits of the above families of holomorphic discs and, assuming regularity (proven in section 5.4), we argue that the disc counts are the same for X_0 and X_t for a sufficiently small t. Lemma 5.3.2 will allow us to prove:

Proposition 5.3.3. *For all $I \subset \{1, 2, 3, 4, 5\}$ and $\theta \in \mathbb{R}$, the discs described by (5.17) uniformly converge to discs contained in the complement of the orbifold point of $\mathbb{CP}(1, 1, 4)$, described in the coordinates $(\tilde{x} : \tilde{y} : \tilde{z})$ by*

$$\tilde{x}(w) = e^{-i\theta}\sqrt{rw^5 + c}\prod_{\substack{j \notin I \\ j \neq 0}}\tau_j(w); \ \tilde{y}(w) = w; \ \tilde{z}(w) = e^{i\theta}\sqrt{rw^5 + c}\prod_{j \in I}\tau_j(w), \tag{5.20}$$

where $\tau_j = \tau_{-\frac{r^{\frac{1}{5}}}{c}e^{\frac{2\pi i}{5}j}}$. For each I and θ, we denote this disc by u_I^θ. Moreover, the algebraic count of discs in the relative class $[u_I^\theta]$, for $|I| = 0, 1, 2, 3, 4, 5$ is equal to $1, 5, 10, 10, 5, 1$, up to sign, respectively.

Proof. (*of Lemma* 5.3.2)

Consider the polynomial:

$$
\begin{aligned}
\Xi(w) &= w^3(1 - \bar{b}w)(w - \nu)^3 \Psi(w) \\
&= r(w - b)(1 - \bar{\nu}w)^3 + cw^3(1 - \bar{b}w)(w - \nu)^3 \qquad (5.21) \\
&= -c\bar{b}(w - \zeta) \prod_j (w - \eta_j), \qquad (5.22)
\end{aligned}
$$

where $|\zeta| > 1$, and write

$$
\prod_j (w - \eta_j) = w^6 - \sigma_1 w^5 + \sigma_2 w^4 - \sigma_3 w^3 + \sigma_4 w^2 - \sigma_5 w + p.
$$

Comparing the coefficients of 1 and w^6, we get:

$$
p\zeta = -\frac{rb}{c\bar{b}}, \qquad (5.23)
$$

$$
1 + 3\nu\bar{b} = \bar{b}(\zeta + \sigma_1). \qquad (5.24)
$$

For the following we recall that $h^2(w) = \frac{\Psi(w)w^3\tau_\nu^3(w)}{\prod \tau_j(w)}$, in particular, by (5.16), $h^2(0) = -\frac{rb}{p}$ and $h^2(\nu) = \frac{r\tau_b(\nu)}{\prod_j q_j}$.

By (5.23), (5.24), and noting that $|\sigma_1 - 3\nu| \leq |\sigma_1| + 3|\nu| \leq 9 \leq 9|\zeta|$, we get that:

$$
1 = |b||\zeta + \sigma_1 - 3\nu| \leq 10|\bar{b}||\zeta| = 10\frac{|h(0)|^2}{c}.
$$

So $|h(0)|^2 \geq \frac{c}{10}$, proving the first statement of Lemma 5.3.2. We see from (5.18) that $\prod_{j \notin I} \eta_j^2 = O(t)$ and hence $p = O(t^{\frac{1}{2}}) \to 0$ as $t \to 0$. Also $\zeta \to \infty$, $b = O(t^{1/2}) \to 0$ and $\bar{b}\zeta = 1 + O(t^{\frac{1}{2}}) \to 1$.

Now we basically need to show that $\nu = O(t^{1/2})$, since the asymptotic behavior of the η_j's described in Lemma 5.3.2 follows from (5.21) and $\nu = O(t^{1/2})$, after we separete the terms that are $O(t^{1/2})$, more precisely, $\Xi(w) = w(r + cw^5) + w^7 O(t^{1/2}) + O(t^{1/2})$. So, let's look to $\Xi(\nu)$ using (5.21) and (5.22) (recall that $q_j = \tau_j(\nu) = (\nu - \eta_j)/(1 - \bar{\eta}_j\nu)$:

$$
\begin{aligned}
\Xi(\nu) &= r(1 - |\nu|^2)^3(\nu - b) \\
&= -c\bar{b}(\nu - \zeta) \prod_j (\nu - \eta_j) = -c\bar{b}(\nu - \zeta) \prod_j q_j(1 - \bar{\eta}_j\nu) \qquad (5.25)
\end{aligned}
$$

Claim 5.3.4. *$h(\nu)$ is bounded away from 0, and by (5.19), $\prod_{j \notin I} q_j^2 = O(t)$, and therefore $\prod_j q_j = O(t^{1/2})$.*

Proof. Using that $\bar{b}\zeta = 1 + O(t^{1/2})$ and $\bar{b}\nu = O(t^{1/2})$ we see that

$$h^2(\nu) = \frac{r\tau_b(\nu)}{\prod_j q_j} = \frac{r(\nu - b)}{\prod_j q_j} \frac{1}{1 - \nu\bar{b}} = \frac{c\prod_j(1 - \bar{\eta}_j\nu)}{(1 - |\nu|^2)^3(1 - \nu\bar{b})}(1 + O(t^{1/2}))$$

is bounded away from zero. Indeed, if $\frac{c\prod_j(1-\bar{\eta}_j\nu)}{(1-|\nu|^2)^3(1-\nu\bar{b})}$ approaches zero, then, since $c\bar{b}(\nu - \zeta)\prod_j q_j$ is bounded, we get by (5.25) that $b - \nu \to 0$ and hence $\nu \to 0$. But in this case we see that $\prod_j(1 - \bar{\eta}_j\nu) \to 1$, not 0.

Then we see from (5.19) that $\prod_{j \notin I} q_j^2 = O(t)$, hence $\prod_j q_j = O(t^{1/2})$. $\square$

We want to show that $b - \nu \to 0$ and hence $\nu \to 0$. For that to follow from (5.25) and Claim 5.3.4, we need to see that $|\nu|$ does not approach 1 as $t \to 0$.

Claim 5.3.5. *As* $t \to 0$, $|\nu|$ *is bounded by a constant strictly smaller than* 1.

Proof. Let's look again to $\Xi(w)$, knowing that $b = O(t^{1/2})$:

$$\Xi(w) = rw(1 - \bar{\nu}w)^3 + cw^3(w - \nu)^3 + w^7 O(t^{1/2}) + O(t^{1/2}) \tag{5.26}$$

Then we see that the roots η_j lying inside the disc are very close to the solutions of $rw(1 - \bar{\nu}w)^3 + cw^3(w - \nu)^3 = 0$, for t very small. The non-zero solutions satisfy:

$$|w^2\tau_\nu(w)^3| = \frac{r}{c} < 1. \tag{5.27}$$

Now, assume there is a sequence of values of t tending to 0 and holomorphic discs such that $\nu \to \nu_0$, $|\nu_0| = 1$. From equation (5.26), we conclude that three of the roots η_j of $\Xi(w)$ converge to ν_0, say η_1, η_2, η_3, one converges to 0, say η_0, and the other two solutions, η_4 and η_5 converge to square roots of $\frac{r}{c\nu_0^3}$, by (5.27) (for values of w lying outside a neighborhood of ν_0, $\tau_\nu(w) = \frac{w-\nu}{1-\bar{\nu}w} = -\nu\frac{1-\nu^{-1}w}{1-\bar{\nu}w} \to -\nu_0$).

Let ϵ_j be such that $\eta_j = \nu - \epsilon_j$, for $j = 1, 2, 3$. By (5.25), recalling that $b = O(t^{1/2})$, $\prod_j q_j = O(t^{1/2})$ and $\bar{b}\zeta = 1 + O(t^{1/2})$ we see that $(1 - |\nu|^2)^3 = K\epsilon_1\epsilon_2\epsilon_3$, where

$$K = \frac{-c\bar{b}(\nu - \zeta)(\nu - \eta_0)}{r(\nu - b)}(\nu - \eta_4)(\nu - \eta_5) \to \frac{c}{r}\nu_0 - \frac{1}{\nu_0^4}$$

is bounded above and below.

Since $\prod_j q_j = O(t^{1/2})$, some $q_j \to 0$, for $j = 1, 2, 3$. Up to relabeling, assume $q_1 \to 0$. We have that, for $j = 1, 2, 3$:

$$q_j = \tau_j(\nu) = \frac{\nu - \eta_j}{1 - \bar{\eta}_j\nu} = \frac{\epsilon_j}{1 - |\nu|^2 + \nu\bar{\epsilon}_j}. \tag{5.28}$$

So,

$$\frac{1}{q_1} = \left(\frac{1 - |\nu|^2}{\epsilon_1}\right) + \nu\frac{\bar{\epsilon}_1}{\epsilon_1} = \left(\frac{K\epsilon_2\epsilon_3}{\epsilon_1^2}\right)^{\frac{1}{3}} + \nu\frac{\bar{\epsilon}_1}{\epsilon_1} \to \infty. \tag{5.29}$$

Passing to a subsequence if needed, we may assume that $|\epsilon_1| \le |\epsilon_2| \le |\epsilon_3|$. So by (5.29), $\frac{\epsilon_1}{\epsilon_3} \to 0$. Therefore,

$$\left| \frac{1}{q_3} \right| = \left| \left(\frac{K\epsilon_1 \epsilon_2}{\epsilon_3^2} \right)^{\frac{1}{3}} + \nu \frac{\bar{\epsilon}_3}{\epsilon_3} \right| \to |\nu_0| = 1. \tag{5.30}$$

But, by (5.27) and $|\tau_{\eta_j}(\nu)| = |\tau_\nu(\eta_j)|$, $|\eta_3|^2 |q_3|^3 \to \frac{r}{c}$, which gives a contradiction since $|\eta_3| \to |\nu_0| = 1$ and $|q_3| \to 1$. $\qquad \square$

Using Claim 5.3.5, equation (5.25), $b = O(t^{1/2})$ and $\prod_j q_j = O(t^{1/2})$, we see that $\nu = O(t^{1/2})$.

So $\Xi(w) = w(r + cw^5) + w^7 O(t^{1/2}) + O(t^{1/2})$ and, assuming $|\eta_0| \le |\eta_j| \ \forall j$, we get that for $j \ne 0$, $\eta_j \to -(\frac{r}{c})^{\frac{1}{5}} e^{\frac{j2\pi i}{5}}$, while $\eta_0 = O(t^{1/2})$. This finishes the proof of Lemma 5.3.2. $\qquad \square$

Proof. (of Proposition 5.3.3)

In the limit $t = 0$, taking into account that $b = O(t^{1/2})$, $\nu = O(t^{1/2})$, $\eta_0 = O(t^{1/2})$ and $\eta_j \to -(\frac{r}{c})^{\frac{1}{5}} e^{\frac{j2\pi i}{5}}$, we have that $\Psi(w)$, $\prod_{j=1}^5 \tau_j(w)$, and $h^2(w)$, thought as maps form $\mathbb{D}$ to $\mathbb{CP}^1$, uniformly converge to

$$\Psi(w) = \frac{r + cw^5}{w^5}; \quad \prod_{j=1}^5 \tau_j(w) = \frac{cw^5 + r}{rw^5 + c}; \quad h^2(w) = rw^5 + c.$$

So, for instance, in the case $I = \{1, 2, 3, 4, 5\}$ we get that $z_1(w)$, $z_2(w)$, $z_3(w)$ uniformly converge to

$$z_1(w) = w^2; \quad z_2(w) = e^{-i\theta} w \sqrt{rw^5 + c}; \quad z_3(w) = e^{i\theta} \frac{cw^5 + r}{rw^5 + c} \sqrt{rw^5 + c};$$

$$z_0(w) = \frac{z_2^2(w)}{z_1(w)} = e^{-2i\theta}(rw^5 + c).$$

Hence using the $(\tilde{x} : \tilde{y} : \tilde{z})$ coordinates of $\mathbb{CP}(1, 1, 4)$ we have

$$\tilde{x}(w) = e^{-i\theta} \sqrt{rw^5 + c}; \quad \tilde{y}(w) = w; \quad \tilde{z}(w) = e^{i\theta} \sqrt{rw^5 + c} \frac{cw^5 + r}{rw^5 + c}.$$

In general, for each I, the holomorphic discs uniformly converge to discs u_I^θ given by

$$\tilde{x}(w) = e^{-i\theta} \sqrt{rw^5 + c} \prod_{\substack{j \notin I \\ j \ne 0}} \tau_j(w); \quad \tilde{y}(w) = w; \quad \tilde{z}(w) = e^{i\theta} \sqrt{rw^5 + c} \prod_{j \in I} \tau_j(w).$$

Note that none of these discs pass through the singular point $(0 : 0 : 1)$ of $\mathbb{CP}(1, 1, 4)$.

As before, we have extra automorphisms of the disc, given by $w \mapsto e^{ik\frac{2\pi}{5}} w$ that don't change (5.16) and we need to quotient out by this action of $\mathbb{Z}/5\mathbb{Z}$. We get that $k \in \mathbb{Z}_5$ acts on u_I^θ as follows:

$|I|$	0	1	2	3	4	5
$u^\theta_I \mapsto$	$u^{\theta+k\frac{2\pi}{5}}_\emptyset$	$u^{\theta+2k\frac{2\pi}{5}}_{I-k}$	$u^{\theta+3k\frac{2\pi}{5}}_{I-k}$	$u^{\theta+4k\frac{2\pi}{5}}_{I-k}$	u^θ_{I-k}	$u^{\theta+k\frac{2\pi}{5}}_I$

where $I - k = \{l \in \{1, \ldots, 5\} : l \equiv j - k \mod 5, \ j \in I\}$.

We also note that, for fixed I, varying $\theta \in [0, 2\pi]$ and looking at the boundary of the discs, the 2-cycle swept by ∂u^θ_I is $[\partial u^\theta_I] = \pm 5[T^c_{r,0}]$. Therefore, in the case $|I| = 0$ or 5, after quotienting by $\mathbb{Z}/5\mathbb{Z}$, the algebraic count is ± 1. In the cases $|I| = 1$ or 4, the action of $\mathbb{Z}/5\mathbb{Z}$ permutes the indices, so the moduli space of holomorphic discs is given by $\{u^\theta_I; \theta \in [0, 2\pi]\}$, where $I = \{1\}$, respectively $I = \{2, 3, 4, 5\}$, hence the algebraic count is ± 5. Similarly for $|I| = 2$ or 3, the action of $\mathbb{Z}/5\mathbb{Z}$ permutes the indices, so the moduli space of holomorphic discs is given by $\{u^\theta_I; \theta \in [0, 2\pi]\} \cup \{u^\theta_{I'}; \theta \in [0, 2\pi]\}$, where $I = \{1, 2\}$ and $I' = \{1, 3\}$, respectively $I = \{3, 4, 5\}$, $I' = \{2, 4, 5\}$, hence the algebraic count is ± 10. $\qquad \square$

Lemma 5.3.6. *Assuming regularity, each of the above families of discs in X_0 has a corresponding family in X_t, for a sufficiently small t.*

Proof. We consider the 3-dimensional complex hypersurface $\mathcal{X}$ inside $\mathbb{C} \times (\mathbb{CP}(1, 1, 1, 2) \setminus (0 : 0 : 0 : 1))$ defined by the equation

$$\mathcal{X} : z_0 z_1 - (1 - t) z_2^2 - t z_3 = 0 \tag{5.31}$$

containing

$$\mathcal{L} = \left\{ (t, (z_0 : z_1 : z_2 : z_3)); t \in \mathbb{R} \ \text{ and } \ \left| \frac{z_2 z_3}{z_1^3} - c \right| = r; \left| \frac{z_2}{z_1} \right|^2 = \left| \frac{z_3}{z_1^2} \right|^2 \right\} \tag{5.32}$$

as a totally real submanifold.

Then we consider $\mathcal{M}(\mathcal{X}, \mathcal{L})$ the moduli space of Maslov index 2 holomorphic discs in $\mathcal{X}$ with boundary on $\mathcal{L}$. By applying the maximum principle to the projection on the first factor, we see that such holomorphic discs lie inside the fibers X_t, for $t \in \mathbb{R}$. Let's consider discs that stay away from the singular point in X_0, such as those computed above.

Assuming the discs above are regular in X_0 implies they are regular as discs in $\mathcal{X}$. This follows from the splitting $u^* T\mathcal{X} = u^* TX_0 \oplus \mathbb{C}$ and the $\bar{\partial}$ operator being surjective onto 1-forms with values in $u^* TX_0$, by the assumed regularity, and onto 1-forms with values in $\mathbb{C}$, by regularity of holomorphic discs in $\mathbb{C}$ with boundary in $\mathbb{R}$.

Hence $\mathcal{M}(\mathcal{X}, \mathcal{L})$ is smooth near the solutions for $t = 0$ given above and the map $\mathcal{M}(\mathcal{X}, \mathcal{L}) \to \mathbb{R}$, which takes a disc in the fiber X_t to t, is regular at 0. Therefore for a small t, all the Maslov index 2 holomorphic discs in X_0 computed above deform to holomorphic discs in X_t. $\qquad \square$

The regularity of the discs above is proven in Theorem 5.4.4.

The families of discs in the classes $2H - 5\beta + k\alpha$, given by (5.17) have been shown to converge uniformly to the corresponding ones in $\mathbb{CP}(1, 1, 4)$ given by (5.20). Smoothness of

the moduli space $\mathcal{M}(\mathcal{X}, \mathcal{L})$ near the families of discs given by (5.20) in X_0 guarantees that each family $\{u^\theta_I; \theta \in [0, 2\pi]\}$ has a unique family in X_t converging to it, for all t sufficiently small. Hence the counts of Maslov index 2 holomorphic discs in the classes $2H - 5\beta + k\alpha$ for X_t are the same as the ones computed in X_0. This finishes the proof of Theorem 5.3.1. $\square$

5.4   Regularity

In order to prove regularity, we consider the following two lemmas.

Lemma 5.4.1. *Let u_θ be a one parameter family of Maslov index 2 holomorphic discs in a Kähler 4 dimensional manifold X with boundary on a Lagrangian L. Set $u = u_0$ and $V = \frac{\partial}{\partial\theta}u_\theta\big|_{\theta=0}$ a vector field along u, tangent to TL along the boundary of u.*
  If V is nowhere tangent to $u(\mathbb{D})$ and $u : \mathbb{D} \to X$ is an immersion, then u is regular.

Proof. As u is an immersion, we can consider the splitting $u^*TX \cong T\mathbb{D} \oplus \mathfrak{L}$ as holomorphic vector bundles, where $\mathfrak{L}$ is the trivial line bundle generated by V. Also $u^*_{|S^1}TL \cong TS^1 \oplus Re(\mathfrak{L})$, where $Re(\mathfrak{L}) = \mathrm{span}_\mathbb{R}\{V\}$ and $S^1 \cong \partial\mathbb{D}$.
  So a section $\zeta \in \Omega^0_{u^*_{|S^1}TL}(\mathbb{D}, u^*TX)$ of u^*TX that takes values in $u^*_{|S^1}TL$ along the boundary splits as $\zeta_1 \oplus \zeta_2 \in \Omega^0_{TS^1}(\mathbb{D}, T\mathbb{D}) \oplus \Omega^0_{Re(\mathfrak{L})}(\mathbb{D}, \mathfrak{L})$. Since J is an integrable complex structure, the kernel of the linearized operator $D_{\bar\partial}$ is given by

$$\{\zeta \in \Omega^0_{u^*_{|S^1}TL}(\mathbb{D}, u^*TX); \bar\partial\zeta = 0\}$$

which is isomorphic to

$$\{\zeta_1 \in \Omega^0_{TS^1}(\mathbb{D}, T\mathbb{D}); \bar\partial\zeta_1 = 0\} \quad \oplus \quad \{\zeta_2 \in \Omega^0_{Re(\mathfrak{L})}(\mathbb{D}, \mathfrak{L}); \bar\partial\zeta_2 = 0\}$$
$$\cong T_{Id}\mathrm{Aut}(\mathbb{D}) \quad \oplus \quad \mathrm{Hol}((\mathbb{D}, S^1), (\mathbb{C}, \mathbb{R}))$$

The last term on the right comes from $\mathfrak{L}$ being trivial. $\mathrm{Aut}(\mathbb{D})$ is known to be 3 dimensional, while $\mathrm{Hol}((\mathbb{D}, S^1), (\mathbb{C}, \mathbb{R}))$ is the space of real-valued constant functions. Therefore,

$$Dim\mathrm{Ker}(D_{\bar\partial}) = 4 = 2 \cdot \chi(\mathbb{D}) + \mu(u^*TX, u^*_{|S^1}TL) = \mathrm{index}(D_{\bar\partial})$$

$\square$

The following lemma sets a sufficient condition for V, as given in the previous lemma, not to be tangent to $u(\mathbb{D})$.

Lemma 5.4.2. *Let $u : \mathbb{D} \to X$ be a Maslov index 2 holomorphic disc in a Kähler 4-manifold X with boundary on a Lagrangian L such that $u_{S^1} : S^1 \to L$ is an immersion, and V a holomorphic vector field on X along u, tangent to L at the boundary. If V is not tangent to $u(\mathbb{D})$ at the boundary, then u is an immersion and V is nowhere tangent to $u(\mathbb{D})$.*

Proof. Suppose that either $du(x) = 0$ or V is tangent to $u(\mathbb{D})$ at a point $u(x)$; up to reparametrizing the disc we may assume that $x \neq 0$. Consider another holomorphic vector field $W = du(\frac{\partial}{\partial\theta})$ given by an infinitesimal rotation, which is tangent to $u(\mathbb{D})$, has a zero at 0 and is also tangent to L at the boundary. Then the Maslov index can be computed using $\det^2(W \wedge V)$, so the number of zeros of $\det(W \wedge V)$ is $\mu(u^*TX, u|_{\partial\mathbb{D}}TL)/2 = 1$. But W vanishes at $u(0)$ and either vanishes or is parallel, as a complex vector, to V at $u(x)$. Since the zeros of $W \wedge V$ always occur with positive multiplicity, as the vector fields are holomorphic, we get a contradiction.

$\square$

Now we are ready to prove

Theorem 5.4.3. *The holomorphic discs representing the classes β and $H - 2\beta + m\alpha$ in X_t computed on proposition 5.1.1 and theorem 5.2.1 are regular, for small t.*

Proof. By Lemmas 5.4.1, 5.4.2, we only need to notice that for each of the holomorphic discs u^θ_I considered, the vector field $V(w) = \frac{\partial}{\partial\theta}u^\theta_I(w)$ is not tangent to $u^\theta_I(\partial\mathbb{D})$. We note that in the limit $t = 0$, we have that u^θ_I uniformly converge, in a compact neighborhood of the boundary, to a holomorphic disc given by:

$$z_1(w) = w; \quad z_2(w) = e^{-i\theta}\sqrt{rw^2 + c}\prod_{\substack{j\notin I \\ j\neq 0}}\tau_{\eta_j}(w); \quad z_3(w) = e^{i\theta}\sqrt{rw^2 + c}\prod_{j\in I}\tau_{\eta_j}(w)$$

where $\eta_1 = i\sqrt{r/c}$, $\eta_2 = -i\sqrt{r/c}$. So we see that in the limit $t = 0$, $V(w) = \frac{\partial}{\partial\theta}u^\theta_I(w)$ is parallel to the fibers of $f(z_0 : z_1 : z_2 : z_3) = \frac{z_2 z_3}{z_1^3}$ restricted to X_0 and nowhere vanishing. Therefore, $V(w)$ is not tangent to $u^\theta_I(\partial\mathbb{D})$ for $t = 0$, and by continuity the same holds for small t.

$\square$

Theorem 5.4.4. *The holomorphic discs in X_0 computed in Theorem 5.3.1 are regular. By Lemma 5.3.6, for small t, the corresponding holomorphic discs in the classes $2H - 5\beta + m\alpha$ in X_t are also regular.*

Proof. Similar to the other cases, for each considered holomorphic disc u_θ, we have the vector field $V(w) = \frac{\partial}{\partial\theta}u_\theta(w) = (i\tilde{x}(w), -i\tilde{z}(w))$ in coordinates $(\tilde{x}, \tilde{z})$, for $\tilde{y} = 1$ on $\mathbb{CP}(1,1,4)$ along the boundary. These vectors are not tangent to $u_\theta(\mathbb{D})$ along the boundary, since they are nonvanishing and parallel to the fibers of $f(\tilde{x}, \tilde{z}) = \tilde{x}\tilde{z}$. Hence, by lemmas 5.4.1, 5.4.2, these discs are regular. $\square$

5.5   Orientation

The choice of orientation of the moduli space of holomorphic discs is determined by a choice of spin-structure on the Lagrangian; see [7] section 5. In this section we choose a spin structure

on our Lagrangian $T(1, 4, 25)$ torus and argue that, under the choice of orientations made in [10], see also section 7 of [7], the evaluation map from each of the moduli spaces of Maslov index 2 holomorphic discs considered in this section to the $T(1, 4, 25)$ torus is orientation preserving. We use the same definition of spin-structure given by C. Cho in section 6 of [7]:

Definition 5.5.1. *A spin structure on an oriented vector bundle E over a manifold M is a homotopy class of a trivialization of E over the 1-skeleton of M that can be extended over the 2-skeleton.*

In case of surfaces, it's enough to consider a stable trivialization of the tangent bundle. We see that $\partial\alpha$ and $\partial\beta$ form a basis of $H_1(T_{r,0}^c, \mathbb{Z})$ and hence they induce a trivialization of the tangent bundle of $T_{r,0}^c$ oriented as $\{\partial\alpha, \partial\beta\}$.

The orientation of the moduli space at a disc $u : (\mathbb{D}, \partial\mathbb{D}) \to (X^{2n}, L^n)$ is then given by the orientation of the index bundle of the linearized operator $D\bar{\partial}_u$ that is induced by the chosen trivialization of the tangent bundle TL along $\partial\mathbb{D}$, as described in [10].

The rough idea is that we extend the trivialization of the tangent bundle of the Lagrangian to a neighborhood of $\partial\mathbb{D}$, then take a concentric circle contained in it, and pinch it to a point $O \in \mathbb{D}$, the part of the disc inside the circle becoming a $\mathbb{CP}^1$. The trivialization of TL along the pinched neighborhood gives a trivialization of its complexification TX. This way, considering the isomorphisms given by the trivializations, the linearized operator is homotopic to a $\bar{\partial}$ operator on $\mathbb{D} \cup \mathbb{CP}^1$, whose kernel consists of pairs (ξ_0, ξ_1) where: ξ_0 is a holomorphic section of the trivial bundle $\mathbb{C}^n$ over the disc, with boundary on the trivial subbundle $\mathbb{R}^n$, i.e, a constant maps into $\mathbb{R}^n$; and ξ_1 is a holomorphic section of the bundle induced by u^*TX over $\mathbb{CP}^1$, which we denote by $TX|_{\mathbb{CP}^1}$. These sections must match at $O \in \mathbb{D}$ and the 'south pole' $S \in \mathbb{CP}^1$. In other words, Fukaya, Oh, Ohta, Ono show that the index of the linearized operator (seen as a virtual vector space $\mathrm{Ker}D\bar{\partial}_u - \mathrm{CoKer}D\bar{\partial}_u$) is isomorphic to the kernel of the homomorphism:

$$(\xi_0, \xi_1) \in Hol(\mathbb{D}, \partial\mathbb{D} : \mathbb{C}^n, \mathbb{R}^n) \times Hol(\mathbb{CP}^1, TX|_{\mathbb{CP}^1}) \to \xi_0(O) - \xi_1(S) \in \mathbb{C}^n \cong TX|_S \quad (5.33)$$

Now the kernel can be oriented by orienting $\mathbb{R}^n \cong Hol(\mathbb{D}, \partial\mathbb{D} : \mathbb{C}^n, \mathbb{R}^n)$ (which is essentially the trivialization of the tangent space of the Lagrangian), since $Hol(\mathbb{CP}^1, TX|_{\mathbb{CP}^1})$ and $\mathbb{C}^n$ carry complex orientations. For a detailed account of what we just discussed, see Chapter of [10] Part II, also Proposition 5.2 in [7].

Denote by $\tilde{\mathcal{M}}(\gamma)$ the space of holomorphic discs on $\mathbb{CP}^2$ with boundary on $T_{r,0}^c$ in the class γ, not quotiented out by $\mathrm{Aut}(\mathbb{D})$. By the same argument as in section 8 of [7], the factor $\mathbb{R}^n \cong Hol(\mathbb{D}, \partial\mathbb{D} : \mathbb{C}^n, \mathbb{R}^n)$ in (5.33) corresponds to the subspace of $T_u\tilde{\mathcal{M}}(\gamma)$ given by the deformations of u which correspond to translations along the boundary of $T_{r,0}^c$, i.e., generated by $V = \frac{\partial}{\partial\theta}u_\theta$ and by infinitesimal rotations in $\mathrm{Aut}(\mathbb{D})$. This way, we orient the moduli space of discs accordingly with our chosen orientation $\{\partial\alpha, \partial\beta\}$. In particular, $\mathcal{M}(\beta)$, which consists of one-parameter family of discs u_θ described in Proposition 5.1.1, is oriented in the positive direction of θ, since $\frac{\partial u_\theta}{\partial\theta}$ and the tangent vector to the boundary of u_θ form

a positive oriented basis of $TT_{r,0}^c$; while the other moduli spaces $\mathcal{M}(H - 2\beta + m\alpha)$ and $\mathcal{M}(2H - 5\beta + k\alpha)$ are oriented in the negative direction of the parameter θ, since in these cases $\frac{\partial u_\theta}{\partial \theta}$ and the tangent vector to the boundary of u_θ form a negative oriented basis.

Proposition 5.5.2. *The evaluation maps from* $\mathcal{M}_1(\beta)$, $\mathcal{M}_1(H - 2\beta + m\alpha)$ *and* $\mathcal{M}_1(2H - 5\beta + k\alpha)$ *to* $T_{r,0}^c$ *are all orientation preserving.*

Here the subscript 1 refers to the moduli space with one marked point at the boundary. The proof of the proposition above follows from the same argument as in Proposition 8.2 in [7].

As a corollary of all we have done in this section, we get

Theorem 5.5.3. *In the region corresponding to* $T(1, 4, 25)$ *tori, the mirror superpotential is given by* (3.3):

$$W_{T(1,4,25)} = u + 2\frac{e^{-\Lambda}}{u^2}(1 + w)^2 + \frac{e^{-2\Lambda}}{u^5 w}(1 + w)^5$$

Chapter 6

The monotone torus

In this chapter we show that we can modify our symplectic form in a neighborhood of D_5 to a new one for which $T^c_{r,0}$ is Lagrangian monotone. Recall that a Lagrangian L in a symplectic manifold (X, ω) is called monotone if there exists a constant M_L such that for any disc u in $\pi_2(X, L)$ satisfies

$$\int u^* \omega = M_L \mu_L(u)$$

where μ_L is the Maslov class.

Recall the relative homotopy classes $H = [\mathbb{CP}^1]$, β and α defined after Proposition 5.1.1, with Maslov indices $\mu(H) = 6$, $\mu(\beta) = 2$ and $\mu(\alpha) = 0$. A disc in the class α is given by the Lefschetz thimble over the interval $[0, c - r]$ with respect to the symplectic fibration f, so $\int_\alpha \omega = 0$. We see that $L = T^c_{r,0}$ satisfies the monotonicity condition if and only if $[\omega] \cdot \beta = \int_\beta \omega = \Lambda/3$, where $\Lambda = \int_H \omega$.

We could try to compute $\int_\beta \omega$ $(= \int_\beta \tilde\omega)$, which depends on our choice of c and $r < c$. As $r \to 0$, $[\omega] \cdot \beta$ converges to 0. We could take then a very large value for c and r very close to c. Nonetheless, a careful computation shows that the symplectic area $[\omega] \cdot \beta$ remains smaller than $\Lambda/3$. Taking then another approach, we look at table 5.1.4 and see that D_5 intersects β in 2 points and H in 5 points. We can then build a 2-form σ supported in a neighborhood of D_5, so that the ratio $[\sigma] \cdot \beta / [\sigma] \cdot H = 2/5 > 1/3$. By adding a large enough multiple of σ to ω, we get a Kähler form $\hat\omega$ for which $[\hat\omega] \cdot [\beta] = \Lambda/3$.

Proposition 6.0.4. *There is a Kähler form $\hat\omega$ for which $T^c_{r,0}$ is Lagrangian monotone. Moreover, $\hat\omega$ can be chosen to agree with ω away from a neighborhood of D_5 that is disjoint from $T^c_{r,0}$.*

Proof. Take a small enough value of r, for which it is straightforward to see that $[\omega] \cdot \beta < \Lambda/3$. In order to make $T^c_{r,0}$ monotone we perform a Kähler inflation in a neighborhood of the quintic D_5 (see section 5.1) to achieve $[\hat\omega] \cdot \beta = \int_{[\mathbb{CP}^1]} \hat\omega/3$, keeping $[\hat\omega] \cdot \alpha = 0$.

Take a small neighborhood $\mathcal{N}$ of $D_5 = \{s_5 = 0\}$ not intersecting $T^c_{r,0}$, where $s_5 = x\xi^2 - 2cy^2 z\xi + c^2 y^5$. Take a cutoff function χ such that $\chi(|s_5|^2)$ is equal to 1 in a neighborhood of D_5 and is equal to 0 in the complement of $\mathcal{N}$. We then define $\hat\omega = \omega + K\sigma$ for

$$\sigma = \frac{i}{2}\partial\bar{\partial}\log\left(|s_5|^2 + \varepsilon\chi(|s_5|^2)(|x|^2 + |y|^2 + |z|^2)^5\right)$$

where K and ε are constants to be specified. We use the fact that $\partial\bar{\partial}\log(|f|^2) = 0$ for a holomorphic function f, to note that the expression for σ is the same for the homogeneous coordinates $(1 : \frac{y}{x} : \frac{z}{x})$, $(\frac{x}{y} : 1 : \frac{z}{y})$ and $(\frac{x}{z} : \frac{y}{z} : 1)$, therefore σ defines a 2-form on $\mathbb{CP}^2$, and also to note that $\sigma = \partial\bar{\partial}\log(|s_5|^2) = 0$ outside $\mathcal{N}$, so $T^c_{r,0}$ is Lagrangian with respect to $\hat{\omega}$.

Lemma 6.0.5. $[\sigma] = 5[\omega_{FS}]$ *is independent of ε and the cutoff function χ.*

Proof of Lemma. To determine the cohomology class of σ, it is enough to compute $\int_{[\mathbb{CP}^1]}\sigma$. For this we consider $[\mathbb{CP}^1] = \{x = 0\}$, and write $\sigma = \frac{1}{4}dd^c\log\psi_j$, where

$$\psi_1 = \frac{|s_5|^2 + \varepsilon\chi(|s_5|^2)(|x|^2 + |y|^2 + |z|^2)^5}{|y|^{10}},$$

$$\psi_2 = \frac{|s_5|^2 + \varepsilon\chi(|s_5|^2)(|x|^2 + |y|^2 + |z|^2)^5}{|z|^{10}},$$

are homogeneous functions respectively defined on $\{y \neq 0\}$, $\{z \neq 0\}$, such that

$$\frac{\psi_1}{\psi_2} = \frac{|z|^{10}}{|y|^{10}} \tag{6.1}$$

We then divide $[\mathbb{CP}^1] = \{x = 0\}$ into two hemispheres H_+, H_-, contained in $\{y \neq 0\}$, $\{z \neq 0\}$, respectively, to compute

$$
\begin{aligned}
\int_{[\mathbb{CP}^1]}\omega &= \frac{1}{4}\int_{H_+}dd^c\log\psi_1 + \frac{1}{4}\int_{H_-}dd^c\log\psi_2 = \frac{1}{4}\int_{\partial H_+}d^c\log\psi_1 + \frac{1}{4}\int_{\partial H_-}d^c\log\psi_2 \\
&= \frac{1}{4}\int_{\partial H_+}d^c\log\psi_1 - d^c\log\psi_2 = \frac{1}{4}\int_{\partial H_+}d^c\log\left(\frac{|z|^{10}}{|y|^{10}}\right) = \frac{5}{4}\int_{\partial H_+}d^c\log\left(\frac{|z|^2}{|y|^2}\right)
\end{aligned}
\tag{6.2}
$$

which by comparison with the same calculation for ω_{FS} is 5 times the area of $[\mathbb{CP}^1]$ with respect to the Fubini-Study form ω_{FS}. $\qquad\square$

In particular, taking $\varepsilon \to 0$ we get that σ converges to a distribution supported at $D_5 = \{s_5 = 0\}$. Now considering α, β, $H = [\mathbb{CP}^1]$ as cycles in $H_2(\mathbb{CP}^2, \mathbb{CP}^2 \setminus \mathcal{N})$ and $[\sigma] \in H^2(\mathbb{CP}^2, \mathbb{CP}^2 \setminus \mathcal{N})$ we see that their σ-areas are a constant π times their intersection number with D_5, i.e., $\int_\alpha \sigma = \pi\alpha\cdot[D_5] = 0$, $\int_\beta \sigma = \pi\beta\cdot[D_5] = 2\pi$ and $\int_H \sigma = \pi[\mathbb{CP}^1]\cdot[D_5] = 5\pi$.

Then, since the ratio between the σ-area of β and H is $2/5 > 1/3$, we can choose a constant K, so that $[\hat{\omega}]\cdot\beta = [\hat{\omega}]\cdot H/3$. Given this value of K, we can choose ε small enough to ensure that $\hat{\omega}$ is nondegenerate and hence a Kähler form for which $T^c_{r,0}$ is monotone Lagrangian. $\qquad\square$

6.1 The monotone $T(1,4,25)$ torus is exotic

We are now going to prove that the count of Maslov index 2 holomorphic discs is an invariant of monotone Lagrangian submanifolds. We will see that it suffices to show it is an invariant under deformation of the almost complex structure. Let L be a monotone Lagrangian submanifold of a symplectic manifold (X, ω) and J_s, $s \in [0,1]$ a path of almost complex structures such that (L, J_0), (L, J_1) are regular, i.e., for $k = 0, 1$, Maslov index 2 J_k-holomorphic discs are regular. Note that since L is monotone there are no J_s-holomorphic discs of nonpositive Maslov index for any $s \in [0,1]$. Since L is orientable, Maslov indexes are even, so the minimum Maslov index is 2. Therefore, there is no bubbling for Maslov index 2 J_s-holomorphic discs bounded by L, when we vary s.

Consider then, for $\beta \in \pi_2(X, L)$, $\mu(\beta) = 2$, the moduli spaces $\mathcal{M}(\beta, J_s)$ of J_s-holomorphic discs representing the class β, modulo reparametrization. We choose the path J_s generically so that the moduli space

$$\tilde{\mathcal{M}}(\beta) = \bigsqcup_{s=0}^{1} \mathcal{M}(\beta, J_s)$$

is a smooth manifold, with

$$\partial \tilde{\mathcal{M}}(\beta) = \mathcal{M}(\beta, J_0) \cup \mathcal{M}(\beta, J_1).$$

Lemma 6.1.1. *If L is oriented and monotone, the classes and algebraic count of Maslov index 2 J-holomorphic discs with boundary on L are independent of J, as long as (L, J) is regular.*

Proof. Since L is oriented, there is no J-holomorphic discs with odd Maslov index and for L monotone, the Maslov index of a disc is proportional to its area. Hence, Maslov index 2 J-holomorphic discs are the ones with minimal area, for any almost complex structure J. L. Lazzarini ([16]) and Kwon-Oh ([15]) proved that for any J-holomorphic disc u with $u(\partial \mathbb{D}) \subset L$, there is a somewhere injective J-holomorphic disc v, with $v(\mathbb{D}) \subset u(\mathbb{D})$. Therefore, by minimality of area, Maslov index 2 discs are somewhere injective. By connectedness of the space of compatible almost complex structures we can consider J_s, $s \in [0,1]$ a generic path of almost complex structures such that (L, J_0), (L, J_1) are regular as above. The result follows immediately from the cobordism $\tilde{\mathcal{M}}(\beta)$ between $\mathcal{M}(\beta, J_0)$ and $\mathcal{M}(\beta, J_1)$. $\square$

Theorem 6.1.2. *If L_0 and L_1 are symplectomorphic monotone Lagrangian submanifolds of a symplectic manifold (X, ω), with an almost complex structure J so that (L_0, J) and (L_1, J) are regular, then algebraic counts of Maslov index 2 J-holomorphic discs, and in particular the numbers of different classes bounding such discs, are the same.*

Proof. Let $\phi : X \to X$ be a symplectomorphism with $\phi(L_1) = L_0$. Apply Lemma 6.1.1 with $L = L_0$, $J_0 = J$, $J_1 = \phi_* J$. $\square$

Corollary 6.1.3. *The monotone $T(1,4,25)$ torus is not symplectomorphic to either the monotone Chekanov torus or the monotone Clifford torus.*

Remark 6.1.4. *We can try to find an exotic torus in $\mathbb{C}^2$ by considering the $T(1,4,25)$ torus in affine charts. If we restrict to the coordinate charts $\{y \neq 0\}$ or $\{z \neq 0\}$, only the discs in the class β remain. Hence we cannot distinguish the $T(1,4,25)$ torus, considered in the charts $\{y \neq 0\}$ or $\{z \neq 0\}$, from the usual Chekanov torus, which also bounds a single family of holomorphic discs in $\mathbb{C}^2$. In the $\{x \neq 0\}$ coordinate chart, another family of holomorphic discs in the class $2H - 5\beta - \alpha$ remains present, besides the one in the class β. This can be checked directly or just by observing that the intersection numbers of the complex line $\{x = 0\}$ with H, β, α are 1 , 0 and 2, respectively. Therefore our methods cannot distinguish the $T(1,4,25)$ torus, considered in the chart $\{x \neq 0\}$, from the usual Clifford torus in $\mathbb{C}^2$, which also bounds two families of Maslov index 2 holomorphic discs in $\mathbb{C}^2$, whose boundaries also generate the first homology group of the torus.*

6.2 Floer Homology and non-displaceability

The modern way to show that a Lagrangian submanifold L of a symplectic manifold X is non-displaceable by Hamiltonian diffeomorphisms is to prove that its Floer homology $HF(L,L)$ is non-zero. The version of Floer Homology we use in this section to prove that $HF(T_{r,0}^c) \neq 0$ (for some choice of local system) is the Pearl Homology, introduced by Oh in [18]. Here we will follow the definitions and notation similar to the ones given in [3,4].
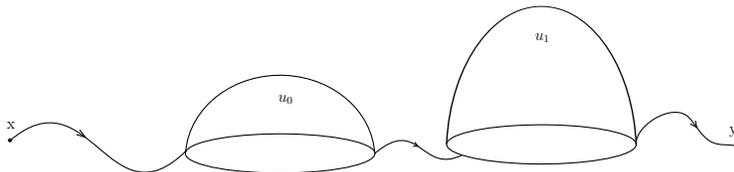
Figure 6.1: A trajectory contributing to the differential of the pearl complex

Let (X, ω) be a symplectic manifold, J a generic almost complex structure compatible with ω, and L a monotone Lagrangian submanifold, with monotonicity constant M_L. We also choose a $\mathbb{C}^*$ local system over L (we don't need to use the Novikov ring because L is monotone, so the area of holomorphic discs is proportional to the Maslov index) and a spin structure to orient the appropriate moduli spaces of holomorphic discs. To define the pearl complex we fix a Morse function $f : L \to \mathbb{R}$ and a metric ρ so that (f, ρ) is Morse-Smale and we denote the gradient flow by γ.

The pearl complex $\mathcal{C}(L; f, \rho, J) = (\mathbb{C}[q, q^{-1}]\langle Crit(f)\rangle, d)$ is generated by the critical points of f, and the differential counts configurations consisting of gradient flow lines of γ together with J-holomorphic discs as illustrated in Figure 6.1. More precisely, for $|x| = ind_f(x)$, $|y| = ind_f(y)$, $B \in \pi_2(M, L)$, $\delta(x, y, B) = |x| - |y| - 1 + \mu(B)$:

$$dx = \sum_{|y|=|x|-1} \#\mathcal{P}(x,y,0) \cdot y \; + \sum_{\substack{\delta(x,y,B)=0, \\ B \neq 0}} (-1)^{|y|} \#\mathcal{P}(x,y,B)\mathrm{hol}_\nabla(\partial B)q^{\mu(B)} \cdot y \qquad (6.3)$$

where ∇ is the chosen local system and $\mathcal{P}(x,y,B)$ is the the moduli space of "pearly trajectories", whose elements are gradient flow lines of f from x to y when $B = 0$, and otherwise tuples $(u_0, t_1, u_1, \cdots, t_k, u_k)$, $k \in \mathbb{Z}_{\geq 0}$ so that:

i. For $0 \leq j \leq k$, u_j is a non-constant J-holomorphic disc with boundary on L, up to reparametrization by an automorphism of the disc fixing ± 1.

ii. $\sum_j [u_j] = B$.

iii. For $1 \leq j \leq k$, $t_j \in (0, +\infty)$, and $\gamma_{t_j}(u_{j-1}(1)) = u_j(-1)$.

iv. $\gamma_{-\infty}(u_0(-1)) = x$, $\gamma_{+\infty}(u_k(1)) = y$.

The choice of spin structure on L gives an orientation for the moduli space of holomorphic discs, and together with the orientation of the ascending and descending manifolds of each critical point of f, one can get a coherent orientation for $\mathcal{P}(x,y,B)$. For a detailed account of how to orient the space of pearly trajectories, see appendix A.2.1 of [4].

We have a filtration given by the index of the critical point. For simplicity we write $\mathcal{C}_*(L)$ for $\mathcal{C}_*(L; f, \rho, J)$. Note that $d = \sum_{j \geq 0} \delta_{2j}$, where $\delta_0 : \mathcal{C}_*(L) \to \mathcal{C}_{*-1}(L)$ is the Morse differential of the function f and $\delta_{2j} : \mathcal{C}_*(L) \to \mathcal{C}_{*-1+2j}(L)$ considers only configurations for which the total Maslov index is $2j$. This gives a spectral sequence (the Oh spectral sequence), converging to the Pearl homology, for which the second page is the singular homology of L with coefficients in $\mathbb{C}[q, q^{-1}]$.

Let $\mathcal{L}$ be the space of $\mathbb{C}^*$ local systems in L and consider the 'superpotential' function $W : \mathcal{L} \to \mathbb{C}[q, q^{-1}]$,

$$W(\nabla) = \sum_{\beta, \mu(\beta)=2} n_\beta q^2 \mathrm{hol}_\nabla(\partial\beta) = \sum_{\beta, \mu(\beta)=2} n_\beta z_\beta(\nabla) \qquad (6.4)$$

where $z_\beta(\nabla) = q^{\frac{\int_\beta \omega}{M_L}}\mathrm{hol}_\nabla(\partial\beta) = q^2\mathrm{hol}_\nabla(\partial\beta)$ and n_β is the count of Maslov index two J-holomorphic discs bounded by L in the class β.

Assume also that the inclusion map $H_1(L) \to H_1(X)$ is trivial, so we have that the ring of regular functions on the algebraic torus $\mathcal{L} \cong \mathrm{hom}(H_1(L), \mathbb{C}^*)$ is generated by the coordinates $z_j = z_{\beta_j}(\nabla)$ for relative classes β_j such that $\partial\beta_j$ generates $H_1(L)$.

The following result is the analogue of Proposition 11.1 of [8] (see also section 12 of [8]) in the pearly setting:

Proposition 6.2.1. *Let f be a perfect Morse function. Denote by p the index 0 critical point, by $q_1, \cdots, q_k$ the index 1 critical points, by $\Gamma_1, \cdots, \Gamma_k$, the closure of the stable manifold of $q_1, \cdots, q_k$, respectively, and by $\gamma_1, \cdots, \gamma_k$ the closure of the respective unstable manifolds. Set $z_j = z_{\gamma_j}$. Then*

$$\delta_2(p) = \sum_j \pm z_j \frac{\partial W}{\partial z_j} q_j$$

In particular $\delta_2(p) = 0$ precisely for the local systems corresponding to the critical points of W.

Proof. (*up to choice of orientations*) We note that the only possible pearly trajectories contributing to the coefficient of q_j in $\delta_2(p)$ consist of a holomorphic discs u with $u(-1) = p$ together with a flow line from $u(1)$ ending in q_j, i.e., $u(1) \in \Gamma_j$. Hence,

$$\delta_2(p) = \sum_{\beta, \mu(\beta)=2} \pm n_\beta z_\beta(\nabla) \sum_j ([\partial\beta] \cdot [\Gamma_j]) q_j \tag{6.5}$$

Since $[\gamma_1], \cdots, [\gamma_k]$ form a basis for $H_1(L)$, we can write $[\partial\beta] = \sum_j a_j [\gamma_j]$, where $a_j = [\partial\beta] \cdot [\Gamma_j]$. So $z_\beta(\nabla)$ is a constant multiple of $\prod_j z_j^{a_j}$, therefore (6.5) gives precisely $\delta_2(p) = \sum_j \pm z_j \frac{\partial W}{\partial z_j} q_j$. $\qquad\square$

Corollary 6.2.2. *Consider the monotone $T(1,4,25)$ torus $T_{r,0}^c$, endowed with the standard spin structure and local system ∇ such that $hol_\nabla(\partial\beta) = \frac{9}{4} e^{k\frac{2\pi}{3} i}$, for some $k \in \mathbb{Z}$, and $hol_\nabla(\partial\alpha) = \frac{1}{8}$, where α and β are as defined in section 5.1. Then the Floer homology $HF(T_{r,0}^c, \nabla)$ is non-zero. Therefore $T_{r,0}^c$ is non-displaceable.*

Proof. Since $T_{r,0}^c$ has dimension 2, all the boundary maps δ_{2j} are zero for $j \geq 2$. Hence the pearl homology $HF(T_{r,0}^c, \nabla)$ is the homology of $(H_*(T_{r,0}^c) \otimes \mathbb{C}[q, q^{-1}], \delta_2)$. Writing $u = z_\beta$ and $w = z_\alpha$, the 'superpotential' is given by

$$W_{T(1,4,25)} = u + 2\frac{q^6}{u^2}(1+w)^2 + \frac{q^{12}}{u^5 w}(1+w)^5$$

The result follows from computing the critical points of $W_{T(1,4,25)}$ which are $w = \frac{1}{8}$, $u = \frac{9}{4} e^{k\frac{2\pi}{3} i} q^2$. $\qquad\square$

Remark 6.2.3. *It can be shown that in fact for any monotone Lagrangian torus $\delta_2 = 0$ for the local systems ∇ which are critical points of W, so $HF(T_{r,0}^c, \nabla) \cong H_*(T_{r,0}^c) \otimes \mathbb{C}[q, q^{-1}]$.*

Chapter 7

Prediction for $\mathbb{CP}^1 \times \mathbb{CP}^1$

In this chapter we apply the same techniques of sections 3, 4 to predict the existence of an exotic monotone torus in $\mathbb{CP}^1 \times \mathbb{CP}^1$ bounding 9 families of Maslov index 2 holomorphic discs, hence not symplectomorphic to the Clifford or Chekanov ones.

We use coordinates $((x : w), (y : z))$ on $\mathbb{CP}^1 \times \mathbb{CP}^1$. We smooth two corners of the divisor $\{xwyz = 0\}$. First considering the fibration given by $f_0((x : w), (y : z)) = \frac{xy}{wz}$ and $D_2 = \{\xi = 0\}$, for $\xi = \frac{xy - wz}{2t}$ and t a positive real number, we smooth the corner of $\{xy = 0\}$ to get a new divisor $D_2 \cup \{wz = 0\}$. Then using $f = \frac{z\xi}{wy^2}$, we smooth the corner of $D_2 \cup \{z = 0\}$ and get a new anticanonical divisor $D = f^{-1}(c) \cup \{w = 0\}$, for c a positive real number. Then we consider a similar singular Lagrangian torus fibration on the complement of D. In particular we define the $T(1, 2, 9)$ (see remark 7.0.5) type torus:

Definition 7.0.4. *Given $c > r > 0$ and $\lambda \in \mathbb{R}$,*

$$T_{r,\lambda}^c = \left\{ ((x : w), (y : z)); \left| \frac{z\xi}{wy^2} - c \right| = r; \left| \frac{z}{y} \right|^2 - \left| \frac{\xi}{wy} \right|^2 = \lambda \right\}, \tag{7.1}$$

which is Lagrangian for a symplectic form similar to (4.6).

Remark 7.0.5. *The role of the parameter t in the definition of ξ is less obvious than in the case of $\mathbb{CP}^2$, since here it amounts to a single rescaling. However as in the case of $\mathbb{CP}^2$, its presence is motivated by considerations about degenerations. More precisely the choice of $\xi = \frac{xy - wz}{2t}$ is based on a degeneration of $\mathbb{CP}^1 \times \mathbb{CP}^1$ to $\mathbb{CP}(1, 1, 2)$, which can be embedded inside $\mathbb{CP}^3$; see Proposition 3.1 of [2]. Applying two nodal trades to the standard polytope of $\mathbb{CP}^1 \times \mathbb{CP}^1$ and redrawing the almost toric diagram as in Figure 2.3, we see that the Chekanov torus corresponds to the central fiber of $\mathbb{CP}(1, 1, 2)$, and the torus fiber obtained by lengthening both cuts to pass through the central fiber of $\mathbb{CP}^1 \times \mathbb{CP}^1$ corresponds to the central fiber of $\mathbb{CP}(1, 2, 9)$, therefore we denote it by $T(1, 2, 9)$.*

We then proceed as in section 3 to predict the number of families of Maslov index 2 holomorphic discs this torus should bound, at least for some values of t, c and r.
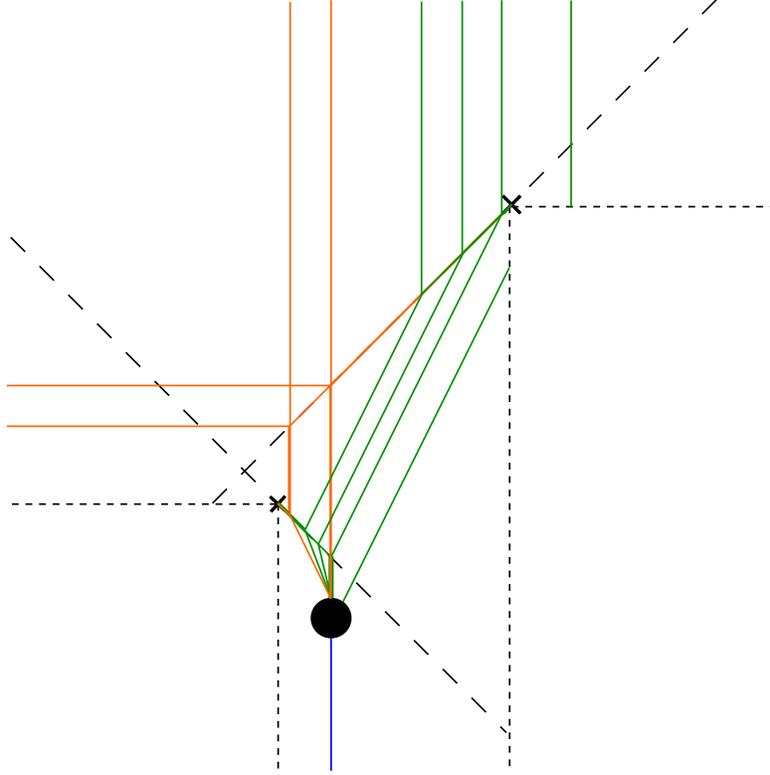
Figure 7.1: A $T(1, 2, 9)$ type torus in $\mathbb{CP}^1 \times \mathbb{CP}^1$ bounding 9 families of Maslov index 2 holomorphic discs. The superpotential is given by $W_{T(1,2,9)} = u_2 + + \frac{e^{-A}}{u_2} + \frac{e^{-B}}{u_2} + \frac{e^{-A}u_1}{u_2^2} + \frac{e^{-B}u_1}{u_2^2} + \frac{e^{-A-B}}{u_1 u_2^2} + 3\frac{e^{-A-B}}{u_2^3} + 3\frac{e^{-A-B}u_1}{u_2^4} + \frac{e^{-A-B}u_1^2}{u_2^5}.$

It is known that the Clifford torus bounds four families of Maslov index 2 holomorphic discs in the classes β_1, β_2, $H_1 - \beta_1$, $H_2 - \beta_2$, where $\beta_1 = [\mathbb{D} \times \{1\}]$ and $\beta_2 = [\{1\} \times \mathbb{D}]$ seen in the coordinate chart $y = 1$, $w = 1$ and $H_1 = [\mathbb{CP}^1] \times \{pt\}$ and $H_2 = \{pt\} \times [\mathbb{CP}^1]$. On the almost toric fibration illustrated on Figure 7.1, it is located in the top chamber and has superpotential given by

$$W_{Clif} = z_1 + z_2 + \frac{e^{-A}}{z_1} + \frac{e^{-B}}{z_2}, \tag{7.2}$$

where z_1 , z_2 are the coordinates associated with β_1, β_2, $A = \int_{[\mathbb{CP}^1] \times \{pt\}} \omega$, $B = \int_{\{pt\} \times [\mathbb{CP}^1]} \omega$. (For a monotone symplectic form $A = B$.)

The first wall-crossing towards the Chekanov type tori gives rise to the change of coordinates $z_1 = v_1(1 + \tilde{w})$, $z_2 = v_2(1 + \tilde{w})^{-1}$, where $\tilde{w} = e^{-A}/z_1 z_2 = e^{-A}/v_1 v_2$. Hence the superpotential becomes

$$W_{Che} = v_2 + v_1(1 + \tilde{w}) + e^{-B}\frac{(1 + \tilde{w})}{v_2} = v_1 + v_2 + \frac{e^{-A}}{v_2} + \frac{e^{-B}}{v_2} + \frac{e^{-A-B}}{v_1 v_2^2}. \qquad (7.3)$$

Crossing now the other wall towards the $T(1, 2, 9)$ type tori, we get the change of coordinates $u_1 = v_1(1 + w)$, $u_2 = v_2(1 + w)$, $w = v_1/v_2 = u_1/u_2$.

The superpotential is then given by

$$
\begin{aligned}
W_{T(1,2,9)} &= u_2 + (e^{-A} + e^{-B})\frac{1 + w}{u_2} + e^{-A-B}\frac{(1 + w)^3}{u_1 u_2^2} \\
&= u_2 + \frac{e^{-A}}{u_2} + \frac{e^{-B}}{u_2} + \frac{e^{-A}u_1}{u_2^2} + \frac{e^{-B}u_1}{u_2^2} \\
&\quad + \frac{e^{-A-B}}{u_1 u_2^2} + 3\frac{e^{-A-B}}{u_2^3} + 3\frac{e^{-A-B}u_1}{u_2^4} + \frac{e^{-A-B}u_1^2}{u_2^5}.
\end{aligned} \qquad (7.4)
$$

7.1   The homology classes

We consider the torus $T_{r,0}^c$. Using notation similar to that in section 5, let's call β the class of the Maslov index 2 holomorphic disc lying on the conic $z = \xi$ that projects into the region $|f - c| \le r$, and α the Lefschetz thimble associated to the critical point of f at the origin lying above the segment $[0, c - r]$ (oriented to intersect positively with $\{z = 0\}$).

As before we use positivity of intersection with some complex curves to restrict the homology classes.

Lemma 7.1.1. *For fixed c and r, for t sufficiently small, the intersection number of the classes α, β, H_1 and H_2 with the varieties $\{x = 0\}$, $\{y = 0\}$, $\{w = 0\}$, $\{z = 0\}$, $D_3 = f^{-1}(c) \cup \{((0 : 1), (1 : 0)), ((1 : 0), (1 : 0))\}$, $D_2 = \{\xi = 0\}$, $D_3' = \{x\xi - cw^2y = 0\}$, $D_6 = D_3 \cup D_3'$ (all of them disjoint from $T_{r,0}^c$) and their Maslov indeces μ, are as giving in the table below:*

Class	$x = 0$	$y = 0$	$w = 0$	$z = 0$	D_2	D_3	D_3'	D_6	μ
α	1	0	0	1	-1	0	0	0	0
β	0	0	0	0	0	1	1	2	2
H_1	1	0	1	0	1	1	2	3	4
H_2	0	1	0	1	1	2	1	3	4

Proof. The intersection numbers of H_1 and H_2 with the given complex curves are computed using Bezout's theorem, and the Maslov index is twice the intersection number with the anticanonical divisor $D = D_3 \cup \{w = 0\}$.

By construction, the intersection of α with $\{z = 0\}$ is one, with D_2 is negative one and with D_3, $\{y = 0\}$ and $\{w = 0\}$ it is clearly zero, as well as the intersection of β and $T_{r,0}^c$ with $\{ywz = 0\}$ and D_2. Also clear is the intersection of β with D_3.

To understand the intersection of the torus $T_{r,0}^c$, α and β with $\{x = 0\}$ and D_3', we look at the family of conics $\mathcal{C} = \{z = e^{i\theta}\xi; \theta \in [0, 2\pi]\}$ containing $T_{r,0}^c$, the thimble representing the class α and holomorphic discs representing the class β, similar to the ones in Proposition (5.1) (for instance one where $z = \xi$, and $Re(z) > 0$). We use the coordinate chart $y = 1$, $w = 1$.

For $\{x = 0\} \cap \mathcal{C}$, we have $z = e^{i\theta}\xi = -e^{i\theta}z/2t$, so the intersection is only at $z = 0$, for t small enough, and with same sign as for $\{z = 0\}$, since x is a multiple of z along $\mathcal{C}$.

For $D_3' \cap \mathcal{C}$, we note that $x = z(2te^{-i\theta} + 1)$ along $\mathcal{C}$. Considering $f = z\xi$, we have

$$0 = x\xi - c = z(2te^{-i\theta} + 1)\xi - c = f(2te^{-i\theta} + 1) - c$$

So, $f = \frac{c}{(2te^{-i\theta}+1)}$, so we see that for t very small, $D_3' \cap \mathcal{C}$ intersects in a circle projecting via f inside the region $|f - c| < r$, therefore D_3' intersects $T_{r,0}^c$, α and β respectively at 0, 0, and 1 point (counting positively as D_3' and our representative of the β class are complex curves). $\square$

Remark 7.1.2. *D_6 was found by considering the degeneration of $\mathbb{CP}^1 \times \mathbb{CP}^1$ to $\mathbb{CP}(1, 1, 2)$ in a similar manner as in section 5.1 D_5 was found using the degeneration of $\mathbb{CP}^2$ to $\mathbb{CP}(1, 1, 4)$. Here it turns out that $D_6 = D_3 \cup D_3'$.*

Lemma 7.1.3. *The only classes in $\pi_2(\mathbb{CP}^1 \times \mathbb{CP}^1, T_{r,0})$ which may contain holomorphic discs of Maslov index 2 are β, $H_1 - \beta$, $H_2 - \beta$, $H_1 - \beta + \alpha$, $H_2 - \beta + \alpha$ and $H_1 + H_2 - 3\beta + k\alpha$, $-1 \leq k \leq 2$.*

Proof. Maslov index 2 classes must be of the form $\beta + k\alpha + m(H_1 - 2\beta) + n(H_2 - 2\beta)$. Considering positivity of intersections with complex curves the proof follows from the inequalities for k, m and n given by the table:

Curve	$x = 0$	$y = 0$	$w = 0$	$z = 0$	D_2	D_3	D_3'
Inequality	$-m \leq k$	$0 \leq n$	$0 \leq m$	$-n \leq k$	$k \leq m + n$	$m \leq 1$	$n \leq 1$

$\square$

7.2   The monotone torus

In order to make $T_{r,0}^c$ a monotone Lagrangian torus, we deform our symplectic form using Kähler inflation in neighborhoods of complex curves that don't intersect $T_{r,0}^c$, in a similar way as we did in section 6. First one can inflate along $\{y = 0\}$ or $\{w = 0\}$ to get a monotone Kähler form $\tilde{\omega}$ for $\mathbb{CP}^1 \times \mathbb{CP}^1$, i.e., $\int_{H_1} \tilde{\omega} = \int_{H_2} \tilde{\omega}$, for which $\int_\alpha \tilde{\omega} = 0$. In order for $T_{r,0}^c$ to be monotone, we need a Kähler form $\hat{\omega}$, satisfying the same conditions as $\tilde{\omega}$ plus $\int_{H_2} \hat{\omega} = 2 \int_\beta \hat{\omega}$. Noting that the intersection numbers of D_6 with α, β, H_1, H_2 are 0 ,2, 3 and 3, respectively, we can get $\hat{\omega}$ by adding a specific multiple of a 2-form supported on a neighborhood of D_6 to $\tilde{\omega}$ as in Proposition 6.0.4, so as to satisfy $\int_\alpha \hat{\omega} = 0$ and $\int_{H_1} \hat{\omega} = \int_{H_2} \hat{\omega} = 2 \int_\beta \hat{\omega}$. The last equality

can be achieved because the ratio between the intersection numbers $[D_6] \cdot H_1 = [D_6] \cdot H_2$ and $[D_6] \cdot \beta$ is $2/3$ which is greater than $1/2$.

Therefore one only need to compute the expected Maslov index 2 holomorphic discs in the classes β, $H_1 - \beta$, $H_2 - \beta$, $H_1 - \beta + \alpha$, $H_2 - \beta + \alpha$ and $H_1 + H_2 - 3\beta + k\alpha$, $-1 \leq k \leq 2$ to prove:

Conjecture 7.2.1. *There is a monotone $T(1, 2, 9)$ torus, of the form $T_{r,0}^c$, in $\mathbb{CP}^1 \times \mathbb{CP}^1$, bounding 9 families of Maslov index 2 holomorphic discs, that is not symplectomorphic to the monotone Chekanov torus nor to the monotone Clifford torus.*

Bibliography

[1]   D. Auroux. *Mirror symmetry and T-Duality on the complement of an anticanonical divisor*, J. Gökova Geom. Topol. GGT 1 (2007), 51-91,

[2]   D. Auroux. *Special Lagrangian fibrations, wall-crossing, and mirror symmetry*, Surveys in differential geometry. Vol. XIII. Geometry, analysis, and algebraic geometry: forty years of the Journal of Differential Geometry, 1-47, Surv. Differ. Geom., 13, Int. Press, Somerville, MA, 2009.

[3]   P. Biran, O. Cornea. *Quantum structures for Lagrangian submanifolds*, arXiv:math/0708.4221v1 [math.SG], 2007.

[4]   P. Biran, O. Cornea. *Lagrangian topology and enumerative geometry*, Geometry & Topology 16 (2012) 963-1052.

[5]   Y. Chekanov. *Lagrangian tori in a symplectic vector space and global symplectomorphisms*, Math. Z. **223** (1996), 547-559.

[6]   Y. Chekanov, F.Schlenk. *Notes on monotone Lagrangian twist tori*, Electron. Res. Announc. Math. Sci. 17 (2010), 104-121.

[7]   C. Cho. *Holomorphic discs, spin structures and Floer cohomology of the Clifford torus*, Int. Math. Res. Not. 2004, no. 35, 1803-1843.

[8]   C. Cho. Y.-G.Oh *Floer cohomology and disc instantons of Lagrangian torus fibers in Fano toric manifolds*, Asian J. Math. 10 (2006), no. 4, 773-814.

[9]   Y. Eliashberg, L. Polterovich. *The problem of Lagrangian knots in four-manifolds*, Geometric Topology (Athens, 1993), AMS/IP Stud. Adv. Math., Amer. Math. Soc., 1997, pp. 313-327

[10]   K. Fukaya, Y.-G. Oh, H. Ohta, K. Ono. *Lagrangian intersection Floer theory: anomaly and obstruction*, Part I and II, AMS/IP Studies in Advanced Mathematics, 46.1. American Mathematical Society, Providence, RI; International Press, Somerville, MA, 2009. xii+396 pp. ISBN: 978-0-8218-4836-4.

[11]   Galkin S., Usnich A., *Mutations of potentials*, Preprint IPMU 10-0100, 2010.

[12]   M. Gross, B. Siebert. *An invitation to toric degenerations*, Surveys in differential geometry. Volume XVI. Geometry of special holonomy and related topics, 43-78, Surv. Differ. Geom., 16, Int. Press, Somerville, MA, 2011.

[13]   P. Hacking, Yu. Prokhorov. *Smoothable del Pezzo surfaces with quotient singularities*, Compos. Math. 146 (2010), no. 1, 169-192.

[14]   M. Kontsevich, Y. Soibelman. *Affine structures and non-archimedean analytic spaces*, The unity of mathematics (P. Etingof, V. Retakh, I.M. Singer, eds.), 321-385, Progr. Math. 244,Birkh auser 2006.

[15]   D. Kwon, Y.-G. Oh. *Structure of the image of (pseudo)-holomorphic discs with totally real boundary condition.*, Appendix 1 by Jean-Pierre Rosay. Comm. Anal. Geom. 8 (2000), no. 1, 3182.

[16]   L. Lazzarini. *Existence of a somewhere injective pseudo-holomorphic disc.*, Geom. Funct. Anal. 10 (2000), no. 4, 829862.

[17]   N.C. Leung, M. Symington, *Almost toric symplectic four-manifolds*, Journal of symplectic geometry Volume 8, Number 2, 143-187, 2010.

[18]   Y.-G. Oh. *Relative Floer and quantum cohomology and symplectic topology of Lagrangian submanifolds*, C.B. Thomas, editor, *Contact and symplectic geometry*, volume 8 of *Publications of Newton institute*, pages 201-267. Cambridge Univ. Press, Cambridge, 1996.

[19]   M. Symington, *Four dimensions from two in symplectic topology*, in Proceedings of the 2001 Georgia International Topology Conference, Proceedings of Symposia in Pure Mathematics, Amer. Math. Soc., Providence, RI, 2003, 153-208.

[20]   N. A. Tyurin *Exotic Chekanov tori in toric symplectic varieties*, IOP Publishing, Journal of Physics: Conference Series 411 (2013) 012028